Fraunhofer
ITWM

M. Buck, O. Iliev, H. Andrä

Multiscale finite element coarse spaces for the analysis of linear elastic composites

Berichte des Fraunhofer ITWM, Nr. 212 (2012)

ISSN 1434-9973

Bericht 212 (2012)

Die Veröffentlichungen in der Berichtsreihe des Fraunhofer ITWM können bezogen werden über:

Fraunhofer-Institut für Techno- und
Wirtschaftsmathematik ITWM
Fraunhofer-Platz 1

67663 Kaiserslautern
Germany

Telefon: +49(0)631/31600-4674
Telefax: +49(0)631/31600-5674
E-Mail: presse@itwm.fraunhofer.de
Internet: www.itwm.fraunhofer.de

Vorwort

Das Tätigkeitsfeld des Fraunhofer-Instituts für Techno- und Wirtschaftsmathematik ITWM umfasst anwendungsnahe Grundlagenforschung, angewandte Forschung sowie Beratung und kundenspezifische Lösungen auf allen Gebieten, die für Techno- und Wirtschaftsmathematik bedeutsam sind.

In der Reihe »Berichte des Fraunhofer ITWM« soll die Arbeit des Instituts kontinuierlich einer interessierten Öffentlichkeit in Industrie, Wirtschaft und Wissenschaft vorgestellt werden. Durch die enge Verzahnung mit dem Fachbereich Mathematik der Universität Kaiserslautern sowie durch zahlreiche Kooperationen mit internationalen Institutionen und Hochschulen in den Bereichen Ausbildung und Forschung ist ein großes Potenzial für Forschungsberichte vorhanden. In die Berichtreihe werden sowohl hervorragende Diplom- und Projektarbeiten und Dissertationen als auch Forschungsberichte der Institutsmitarbeiter und Institutsgäste zu aktuellen Fragen der Techno- und Wirtschaftsmathematik aufgenommen.

Darüber hinaus bietet die Reihe ein Forum für die Berichterstattung über die zahlreichen Kooperationsprojekte des Instituts mit Partnern aus Industrie und Wirtschaft.

Berichterstattung heißt hier Dokumentation des Transfers aktueller Ergebnisse aus mathematischer Forschungs- und Entwicklungsarbeit in industrielle Anwendungen und Softwareprodukte – und umgekehrt, denn Probleme der Praxis generieren neue interessante mathematische Fragestellungen.

Prof. Dr. Dieter Prätzel-Wolters
Institutsleiter

Kaiserslautern, im Juni 2001

Multiscale Finite Element Coarse Spaces for the Analysis of Linear Elastic Composites

M. Buck [1,2], O. Iliev [1,2,3], H. Andrä [1]

[1] Fraunhofer Institute for Industrial Mathematics (ITWM), Kaiserslautern, Germany
[2] Department of Mathematics, University of Kaiserslautern, Germany
[3] Institute of Mathematics and Informatics, Bulgarian Academy of Sciences, Sofia, Bulgaria

In this work we extend the multiscale finite element method (MsFEM) as formulated by Hou and Wu in [14] to the PDE system of linear elasticity. The application, motivated from the multiscale analysis of highly heterogeneous composite materials, is twofold. Resolving the heterogeneities on the finest scale, we utilize the linear MsFEM basis for the construction of robust coarse spaces in the context of two-level overlapping Domain Decomposition preconditioners. We motivate and explain the construction and present numerical results validating the approach. Under the assumption that the material jumps are isolated, that is they occur only in the interior of the coarse grid elements, our experiments show uniform convergence rates independent of the contrast in the Young's modulus within the heterogeneous material. Elsewise, if no restrictions on the position of the high coefficient inclusions are imposed, robustness can not be guaranteed any more. These results justify expectations to obtain coefficient-explicit condition number bounds for the PDE system of linear elasticity similar to existing ones for scalar elliptic PDEs as given in the work of Graham, Lechner and Scheichl [12]. Furthermore, we numerically observe the properties of the MsFEM coarse space for linear elasticity in an upscaling framework. Therefore, we present experimental results showing the approximation errors of the multiscale coarse space w.r.t. the fine-scale solution.

Keywords: linear elasticity, domain decomposition, multiscale finite elements, robust coarse spaces, rigid body modes, discontinuous coefficients

1 Introduction

Steadily growing demands on the range of application of todays industrial products require more and more frequently the development of innovative, highly-effective composite materials, specifically adapted to their field of application. Virtual material design provides an essential support in the development process of new materials as it substantially reduces costs and time for the construction of prototypes and performing measurements on their properties. Of special interest is the multiscale-analysis of particle reinforces composites. They combine positive features of their components such as e.g. lightweight and high stiffness.

Resolving the material jumps on the finest scale when performing the simulations is of high computational cost. The idea of the multiscale finite element method is to capture small scale features of the solution on coarser grid-levels without accurately resolving all the small scale components. It has been successfully applied to scalar elliptic PDEs with highly oscillating coefficients on multiple scales. Different variations of the method can be found in [14, 15, 16, 9], including their analysis in the homogenization framework. A variational multiscale method for Brinkman's equation in highly porous media is presented in [18], an approach which also incorporates the framework of Domain Decomposition.

Furthermore, multiscale finite element methods are often used for the construction of robust two-level overlapping Domain Decomposition preconditioners for scalar elliptic multiscale PDEs (see [12], [13]). Applications to the Brinkman equation can be found in [8]. Although the capability of the adaption of multiscale finite elements to material studies of highly heterogeneous composites is often referred, to the authors knowledge, their application to the 3D system of linear elasticity has not yet taken place. However, an application of an adaptive local-global multiscale finite element method to a 2D linear elasticity problem is given in [25]. There, an extension of the multiscale finite volume element method presented in [7] for two-phase flow problems is proposed. This method iteratively adapts the current multiscale basis functions by combining an oversampling approach locally and a coarse scale simulation globally. In [25], applications to a structural optimization problem in 2D linear elasticity is given.

Two-level overlapping Domain Decomposition preconditioners for the equations of linear elasticity are observed in several papers. The common feature of each of these works is that the coarse space contains the rigid body modes. E.g., in [29], linear coarse spaces are considered. In [19], coarse spaces are constructed by aggregation techniques. In both works, condition number bounds independent of the mesh parameters are shown for a homogeneous material, with possibly large constants in the estimates. Aggregation methods were originally introduced in [32, 33] for scalar elliptic PDEs and first applied to the linear elasticity system in [34]. Under certain conditions, the smoothed aggregation method promises mesh and coefficient independent condition number bounds for the elasticity system. Aggregation based methods are observed in many other works. E.g. in combination with partition of unity coarse spaces in [27], sharper condition number bounds are given depending on the parameters of the underlying material. In a more recent approach in [6], generalized eigenvalue problems are solved in the overlapping regions of the coarse basis functions.

Further robust methods for solving linear elasticity problems are available in the literature, including multilevel methods studied in [24], and further developed in [20] and [21]. In their work, they construct a purely algebraic multigrid method for linear elasticity problems, based on computational molecules, a new variant of AMGe. Such an approach has been studied earlier for the scalar elliptic case in [23]. A multigrid approach based on a finite difference discretization of the elasticity system has been proposed in [37]. Important works concerning classical AMG methods for linear elasticity are given in [4] and [1].

The outline of the report is as follows. We start with the continuous formulation of the governing PDE system and the discretization on the fine grid in section 2. In section 3 we shortly recapitulate the two-level Additive Schwarz algorithm, followed by introducing the precise structure of the underlying fine and coarse grid in 3D. We recapitulate the multiscale finite element method for scalar elliptic PDEs in section 4. The main requirements on a coarse space for the PDE systems of linear elasticity are stated in section 5, followed by a detailed introduction of the multiscale finite element basis. Section 6 is devoted to numerical results, a short discussion finalizes the report in section 7.

2 Governing Equations and their Discretization

2.1 The Equation of Linear Elasticity

For the sake of simplicity, let $\Omega \subset \mathbb{R}^3$ be a cuboidal domain. We consider a solid body in Ω, deformed under the influence of volume forces f and tension forces t. Assuming a linear elastic material behavior, it is well known that the displacement field u of the body is governed by the linear elasticity system [2]

$$-\mathrm{div}\sigma(u) = f \ \text{ in } \Omega, \tag{1}$$

$$\sigma(u) = \mathrm{C} : \varepsilon(u) \ \text{ in } \Omega, \tag{2}$$

where σ is the stress tensor, the strain tensor ε is given by the symmetric part of the deformation gradient

$$\varepsilon = \varepsilon(u) = \frac{1}{2}\left(\nabla u + \nabla u^T\right).$$

$\mathrm{C} = \mathrm{C}(x), x \in \Omega$ is the 4th order elasticity tensor, it describes the elastic stiffness of the material under mechanical load. The coefficients $c_{ijkl}, 1 \leq i,j,k,l \leq 3$ may contain large jumps within the domain Ω. They depend on the parameters of the particular materials which are enclosed in the composite. The boundary conditions are imposed separately for each component $u_i = u \cdot e^i, i = 1,2,3$ of the vector-field $u : \bar{\Omega} \rightarrow \mathbb{R}^3$. Here, e^i denotes the i-th Cartesian basis vector. We shall assume that $\Gamma = \partial\Omega$ admits the decomposition into two disjoint subsets Γ_{D_i} and Γ_{N_i}, $\Gamma = \overline{\Gamma_{D_i} \cup \Gamma_{N_i}}$ and $\mathrm{meas}(\Gamma_{D_i}) > 0$ for $i \in \{1,2,3\}$. The system given in equation (1) follows the boundary conditions

$$\left.\begin{aligned} u_i &= g_i \ \text{ on } \Gamma_{D_i} \\ \sigma_{ij} n_j &= t_i \ \text{ on } \Gamma_{N_i} \end{aligned}\right\} \qquad i = 1,2,3,$$

where n is the unit outer normal vector on $\partial\Omega$.

The Lamé equation Equation (1) is the general form of the PDE system of anisotropic linear elasticity, which can be simplified when the solid body consists of one or more isotropic materials. In this case, equation (2) can be expressed in terms of the Lamé coefficients $\lambda \in \mathbb{R}$ and $\mu > 0$, which are characteristic constants of the specific material. The stress tensor for an isotropic material simplifies to $\sigma(u) = \lambda \mathrm{tr}(\varepsilon(u))I + 2\mu\varepsilon(u)$. We assume that Ω is divided into two disjoint subdomains Ω^1, Ω^2 such that $\bar{\Omega} = \bar{\Omega}^1 \cup \bar{\Omega}^2$. Each of the domains Ω^i contains an isotropic material with Lamé coefficients (λ_i, μ_i), $i = 1, 2$, i.e. let

$$\lambda(x) = \begin{cases} \lambda_1, \ x \in \Omega^1 \\ \lambda_2, \ x \in \Omega^2 \end{cases} \quad \mu(x) = \begin{cases} \mu_1, \ x \in \Omega^1 \\ \mu_2, \ x \in \Omega^2. \end{cases}$$

Let $\Gamma_{\text{face}} := \bar{\Omega}^1 \cap \bar{\Omega}^2 \setminus \partial\Omega$ denote the interface between the two materials. Under the condition of ideal adhesion, equation (1) simplifies to

$$\mu\Delta u + (\lambda + \mu)\nabla(\nabla \cdot u) = f \ \text{ in } \Omega \backslash \Gamma_{\text{face}}, \tag{3}$$

$$[u] = 0, \ [t] = 0 \text{ on } \Gamma_{\text{face}}. \tag{4}$$

Here, $t_j(u) = \sigma_{ij} n_j$ is the normal component of the stress where n is the unit normal to Γ_{face} pointing into Ω^2. The square brackets denote the discontinuity across Γ_{face}. More precisely, $[u(x_0)] = u^2(x_0) - u^1(x_0)$ where $u^i(x_0) := \lim_{\Omega^i \ni x \to x_0} u(x)$, $i = 1, 2$, is the one sided limit of the vector-field u in $x_0 \in \Gamma_{\text{face}}$. Using the symmetry of the strain- and the stress tensor

$$\varepsilon = \begin{pmatrix} \varepsilon_{11} & \varepsilon_{12} & \varepsilon_{13} \\ \varepsilon_{12} & \varepsilon_{22} & \varepsilon_{23} \\ \varepsilon_{13} & \varepsilon_{23} & \varepsilon_{33} \end{pmatrix}, \ \ \sigma = \begin{pmatrix} \sigma_{11} & \sigma_{12} & \sigma_{13} \\ \sigma_{12} & \sigma_{22} & \sigma_{23} \\ \sigma_{13} & \sigma_{23} & \sigma_{33} \end{pmatrix},$$

the Voigt notation enables a simplified representation of the stiffness tensor C in terms of a 6×6 matrix $\tilde{\mathrm{C}}$. The entries of the strain tensor σ in equation (2) can be computed from $(\sigma_{11}, \sigma_{22}, \sigma_{33}, \sigma_{23}, \sigma_{13}, \sigma_{12})^T = \tilde{\mathrm{C}}(\varepsilon_{11}, \varepsilon_{22}, \varepsilon_{33}, 2\varepsilon_{23}, 2\varepsilon_{13}, 2\varepsilon_{12})^T$. For an isotropic material, the stiffness tensor $\tilde{\mathrm{C}}$ in Voigt notation takes the form

$$\tilde{\mathrm{C}} = \begin{pmatrix} 2\mu + \lambda & \lambda & \lambda & & & \\ \lambda & 2\mu + \lambda & \lambda & & 0 & \\ \lambda & \lambda & 2\mu + \lambda & & & \\ & & & \mu & & \\ & 0 & & & \mu & \\ & & & & & \mu \end{pmatrix}.$$

The Lamé coefficients can also be expressed in terms of the Young's modulus $E > 0$ and the Poisson ratio $\nu \in (-1, 1/2)$ by

$$\lambda = \frac{E\nu}{(1+\nu)(1-2\nu)}, \ \ \mu = \frac{E}{2(1+\nu)}. \tag{5}$$

Each pair (E, ν) or (λ, μ) characterizes the properties of an isotropic material. For completeness, we also give the relation

$$E = \frac{\mu(3\lambda + 2\mu)}{\lambda + \mu}, \quad \nu = \frac{\lambda}{2(\lambda + \mu)}.$$

Remark: We should point out here that we only consider compressible linear elastic materials ($\nu < 1/2$), which allows a discretization with piecewise linear (H^1-conforming) finite elements. To circumvent the effect of *locking* or *volume locking*, reasonable discretizations are available when dealing with nearly incompressible materials. Such methods include non-conforming finite elements (c.f. [11], [22]) or a mixed variational formulation by introducing an additional penalty term (c.f. [2], [3]). In our observations, we always assume that the Poisson ratio ν is bounded away from 1/2.

2.2 Weak Formulation

Let the domain $\Omega \subset \mathbb{R}^3$ and $\Gamma_{D_i}, \Gamma_{N_i} \subset \partial\Omega, i = 1, 2, 3$ be defined as in section 2.1. Consider the Sobolev space of square-integrable functions with weak first derivatives in the Lebesgue space $L^2(\Omega)$,

$$H^1(\Omega) = \left\{ f \in L^2(\Omega) \,:\, \partial^s f \in L^2(\Omega) \;\forall\, |s| \leq 1 \right\},$$

equipped with the norm

$$\|f\|_{H^1(\Omega)} := \left(\sum_{|s| \leq 1} \int_\Omega |\partial^s f|^2 dx \right)^{1/2},$$

where $s = (s_1, s_2, s_3) \in \mathbb{N}^3$ is a multi-index with $|s| = s_1 + s_2 + s_3$. We introduce the Sobolev space for vector-fields in $\mathbb{R}^3$ by

$$\mathcal{V} := [H^1(\Omega)]^3 = \left\{ v = (v_1, v_2, v_3)^T : v_i \in H^1(\Omega),\ i = 1, 2, 3 \right\}, \tag{6}$$

$$\mathcal{V}_0 : = \left\{ v \in [H^1(\Omega)]^3 : v_i = 0 \text{ on } \Gamma_{D_i},\ i = 1, 2, 3 \right\} \subset \mathcal{V}. \tag{7}$$

Additionally, we define the manifold

$$\mathcal{V}_g := \left\{ v \in [H^1(\Omega)]^3 : v_i = g_i \text{ on } \Gamma_{D_i},\ i = 1, 2, 3 \right\}. \tag{8}$$

The Sobolev space $\mathcal{V}$ inherits its scalar product from $H^1(\Omega)$, it is given by

$$(u, v)_{[H^1(\Omega)]^3} := \sum_{i=1}^{3} (u_i, v_i)_{H^1(\Omega)}.$$

We assume $f \in \mathcal{V}^{-1}$ to be in the dual space of $\mathcal{V}_0$, $t \in [H^{-\frac{1}{2}}(\Gamma_N)]^3$ is in the trace space and $c_{ijkl} \in L^\infty(\Omega)$ to be uniformly bounded. Additionally, we require the stiffness tensor C to be positive definite, i.e. it holds $(\mathrm{C} : \varepsilon(u)) : \varepsilon(v) \geq C_0\, \varepsilon(u) : \varepsilon(v)$ for a

constant $C_0 > 0$. Note that for an isotropic material with the parameters λ and μ, this condition holds when $C_0/2 < \mu < \infty$ and $C_0 \leq 2\mu + 3\lambda < \infty$. We define the bilinear form $a : \mathcal{V} \times \mathcal{V} \to \mathbb{R}$,

$$a(u, v) := \int_\Omega (\mathrm{C} : \varepsilon(u)) : \varepsilon(v)\, dx. \tag{9}$$

This form is symmetric, continuous, and coercive. The coercivity, i.e.

$$\exists\, c_0 > 0 \ : \ a(v, v) \geq c_0 \left\| v \right\|_{[H^1(\Omega)]^3} \ \ \forall v \in \mathcal{V}_0,$$

can be shown by using Korn's inequality (c.f. [2]). Furthermore, we define the continuous linear form $F : \mathcal{V} \to \mathbb{R}$,

$$F(v) := \int_\Omega f \cdot v\, dx + \int_{\Gamma_N} t \cdot v\, ds.$$

The weak solution of (1) is then given in terms of $a(\cdot, \cdot)$ and $F(\cdot)$ by $u \in \mathcal{V}_g$, such that

$$a(u, v) = F(v)\ \forall v \in \mathcal{V}_0. \tag{10}$$

Under the assumptions above, a unique solution of the weak formulation in equation (10) is guaranteed by the Lax Milgram Lemma [2].

2.3 The Finite Element Discretization

We want to approximate the solution of (10) in a finite dimensional subspace $\mathcal{V}^h \subset \mathcal{V}$. Therefore, let $\mathcal{T}_h$ be a quasi-uniform triangulation of $\Omega \subset \mathbb{R}^3$ into tetrahedral finite elements with mesh parameter h and let $\bar{\Sigma}_h$ be the set of vertices of $\mathcal{T}_h$ contained in $\bar{\Omega}$. We denote the number of grid points in $\bar{\Sigma}_h$ by n_p. In section 3, the regular grid and its triangulation is introduced in more detail. Let $\mathcal{B}^h_{\mathrm{lin}} := \{\varphi_i\}_{i=1}^{n_p}$ be the set of piecewise linear basis functions on the triangulation $\mathcal{T}_h$ of $\bar{\Omega}$, such that

$$\varphi_i(x^j) = \delta_{ij},\ x^j \in \bar{\Sigma}_h.$$

Here, δ_{ij} is the Kronecker delta. We extend the given scalar nodal basis to the space of vector-valued nodal functions on $\bar{\Sigma}_h$ by

$$\mathcal{V}^h := \left\{ v^h \in [C^0(\bar{\Omega})]^3 : v^h_k = \sum_{j=1}^{n_p} \mathrm{v}_{j^{(k)}} \varphi_j,\ \mathrm{v}_{j^{(k)}} \in \mathbb{R},\ k \in \{1, 2, 3\} \right\}. \tag{11}$$

Let e^m denote the m-th Cartesian basis vector in $\mathbb{R}^3$. Then each basis function $\phi_{j^{(m)}} := \varphi_j e^m : \Omega \to \mathbb{R}^3$ of $\mathcal{V}^h$ is a vector-field with a scalar nodal function in one of their components, and zero in the others. For the sake of simplifying the notation, we assume a fixed numbering of the basis functions to be given. To be more specific, we assume the existence of a suitable surjective mapping $\{\phi_{j^{(m)}}\} \to \{1, .., n_d\} \subset \mathbb{N}$, $\phi_{j^{(m)}} \mapsto j^{(m)}$. Note that this mapping automatically introduces a renumbering from

$\{1,..,n_p\} \times \{1,2,3\} \to \{1,..,n_d\}$. Here, $n_d = 3n_p$ denotes the total number of degrees of freedom (DOFs) of $\mathcal{V}^h$. We introduce the discrete analogies to the space in equation (7) and the manifold in equation (8) by

$$\mathcal{V}_0^h := \left\{v^h \in \mathcal{V}^h : v_i^h = 0 \text{ on } \Gamma_{D_i},\, i = 1,2,3\right\}, \tag{12}$$

$$\mathcal{V}_g^h := \left\{v^h \in \mathcal{V}^h : v_i^h = g_i \text{ on } \Gamma_{D_i},\, i = 1,2,3\right\}. \tag{13}$$

We want to find $u^h \in \mathcal{V}_g^h$, where $u^h = w^h + g^h$, with $w^h \in \mathcal{V}_0^h$ and $g^h \in \mathcal{V}_g^h$. More precisely, we seek $u^h = (u_1^h, u_2^h, u_3^h)^T$ with

$$u_k^h = \sum_{j=1}^{n_p} \mathrm{u}_{j^{(k)}} \varphi_j,\ k = 1,2,3,$$

such that

$$a(w^h, v^h) = F(v^h) - a(g^h, v^h)\ \ \forall v^h \in \mathcal{V}_0^h.$$

We define the index set of degrees of freedom of $\mathcal{V}^h$ by $\mathcal{D}^h = \{1,..,n_d\}$ and introduce the subset

$$\mathcal{D}_0^h := \left\{i^{(m)} \in \mathbb{N} : x^i \in \bar{\Sigma}_h,\, x^i \notin \Gamma_{D_m}\right\}.$$

Furthermore, we may introduce $\mathcal{D}_{\Gamma_D}^h := \mathcal{D}^h \backslash \mathcal{D}_0^h \neq \emptyset$. The bilinear form in equation (9) applied to the basis functions of $\mathcal{V}^h$ reads

$$\begin{aligned} a(\phi_{i^{(m)}}, \phi_{j^{(k)}}) &= \int_\Omega \tilde{\varepsilon}(\varphi_i e^m)^T\, \tilde{\mathrm{C}}\, \tilde{\varepsilon}(\varphi_j e^k)\, \mathrm{d}x \\ &= \int_\Omega \sum_{r,l=1}^{3} c_{mrkl}\, \partial_l \varphi_j\, \partial_r \varphi_i\, \mathrm{d}x. \end{aligned}$$

We define $A \in \mathbb{R}^{n_d \times n_d}$, $f \in \mathbb{R}^{n_d}$ by

$$A_{i^{(m)} j^{(k)}} = \begin{cases} a(\phi_{i^{(m)}}, \phi_{j^{(k)}}) & \text{if } i^{(m)}, j^{(k)} \in \mathcal{D}_0^h, \\ a(\phi_{i^{(m)}}, \phi_{i^{(m)}}) & \text{if } i^{(m)} = j^{(k)} \in \mathcal{D}_{\Gamma_D}^h, \\ 0 \text{ otherwise} \end{cases}$$

and

$$f_{j^{(k)}} = \begin{cases} F(\phi_{j^{(k)}}) - \sum\limits_{i^{(m)} \in \mathcal{D}_{\Gamma_D}^h} a(\phi_{i^{(m)}}, \phi_{j^{(k)}}) g_m(x^i) & \text{if } j^{(k)} \in \mathcal{D}_0^h, \\ F(j^{(k)}) = a(\phi_{j^{(k)}}, \phi_{j^{(k)}}) g_k(x^j) & \text{if } j^{(k)} \in \mathcal{D}_{\Gamma_D}^h. \end{cases}$$

Observe that common supports of basis functions $\phi_{i^{(m)}}$ and $\phi_{j^{(k)}}$ with $i^{(m)} \in \mathcal{D}_0^h$, $j^{(k)} \in \mathcal{D}_{\Gamma_D}^h$ do not have a contribution to the entries in A. They only contribute to the loadvector $\mathbf{f}$. This leads to the sparse linear system

$$A\mathbf{u} = \mathbf{f} \tag{14}$$

with the symmetric positive definite (s.p.d.) stiffness matrix A. The symmetry of A is inherited from the symmetry of $a(\cdot,\cdot)$ while the positive definiteness is a direct consequence of the coercivity of the bilinear form. Note that in the construction above, the essential degrees of freedom in $\mathcal{D}^h_{\Gamma_D}$ are not eliminated from the linear system. The degrees of freedom related to Dirichlet boundary values are contained in the linear system by strictly imposing $u^h_i = g^h_i$ on $\Gamma_{D_i}, i \in \{1,2,3\}$. The symmetry of the linear system is kept by an adaption of the right-hand side.

2.4 Assembling the Stiffness Matrix

For implementation purposes, we introduce the matrix B_i related to a node x^i by

$$B_i = \begin{bmatrix} \partial_1\varphi_i & 0 & 0 \\ 0 & \partial_2\varphi_i & 0 \\ 0 & 0 & \partial_3\varphi_i \\ 0 & \partial_3\varphi_i & \partial_2\varphi_i \\ \partial_3\varphi_i & 0 & \partial_1\varphi_i \\ \partial_2\varphi_i & \partial_1\varphi_i & 0 \end{bmatrix}.$$

It holds $\tilde{\varepsilon}(\phi_{i^{(m)}}) = B_i e^m$ where $\phi_{i^{(m)}} = \varphi_i e^m$. One can write, at least for $i^{(m)}, j^{(k)} \in \mathcal{D}^h_0$,

$$A_{i^{(m)}j^{(k)}} = e^{mT} \int_\Omega B_i^T \tilde{\mathrm{C}} B_j \,\mathrm{d}x\, e^k. \tag{15}$$

As usual for finite element methods, the stiffness matrix A and the loadvector $\mathbf{f}$ in equation (14) may be assembled by sums of elemental contributions, rather than entry by entry as in equation (15). For each $\tau \in \mathcal{T}_h$, we define the element submatrix

$$\tilde{A}^\tau = \int_\tau B_\tau^T \tilde{\mathrm{C}} B_\tau \,\mathrm{d}x, \tag{16}$$

where the matrix B_τ contains the nodal matrices $B_{\tau_i}, i = 1,..,4$ corresponding to the 4 vertices of τ,

$$B_\tau = [B_{\tau_1}, B_{\tau_2}, B_{\tau_3}, B_{\tau_4}].$$

An adaption of $\tilde{A}^\tau$ is required if the tetrahedral element touches the global boundary where Dirichlet conditions are applied. We introduce

$$A^\tau_{i^{(m)}j^{(k)}} = \begin{cases} \tilde{A}^\tau_{i^{(m)}j^{(k)}} & \text{if } i^{(m)}, j^{(k)} \in \mathcal{D}^h_0, \\ \tilde{A}^\tau_{i^{(m)}i^{(m)}} & \text{if } i^{(m)} = j^{(k)} \in \mathcal{D}^h_{\Gamma_D}, \\ 0 \text{ otherwise} \end{cases} \tag{17}$$

In a similar way, we define the elemental contribution of the load vector by

$$f^\tau_{j^{(k)}} := \begin{cases} F^\tau(\phi_{j^{(k)}}) - \sum\limits_{i^{(m)} \in \mathcal{D}^h_{\Gamma_D}} A^\tau_{i^{(m)}j^{(k)}} g_m(x^i) & \text{if } j^{(k)} \in \mathcal{D}^h_0, \\ F^\tau(j^{(k)}) = A^\tau_{j^{(k)}j^{(k)}} g_k(x^j) & \text{if } j^{(k)} \in \mathcal{D}^h_{\Gamma_D}. \end{cases} \tag{18}$$

The global stiffness matrix as well as the right-hand side are assembled element-wise. For each $\tau \in \mathcal{T}_h$, the following applies:

1. Assemble $A^\tau, \tau \in \mathcal{T}_h$ as described in equation (17) and compute $\mathbf{f}^\tau$ by equation (18). The essential boundary conditions are taken into account.

2. Update the global stiffness matrix respectively force-vector by the computed elementary contributions.

The later step here requires some additional information. The element-matrices A^τ as well as the corresponding element right-hand side are computed based on a local ordering. Their values have to be added to the appropriate locations in the global counterparts. In practice, all the computations are performed on one reference element τ_{ref}. For more details, we refer the reader to [17].

3 Fine and Coarse Grid for the Two-Level Method

We are interested in solving the linear system in equation (14) and hence, the construction of preconditioners for A which remove the ill-conditioning due to mesh-parameters and variations in the PDE coefficients. Such preconditioners involve corrections on local subdomains as well as a global solve on a coarse grid. Specifically, we apply the two-level Additive Schwarz preconditioner, which we shortly recapitulate in this section. Furthermore, we precisely introduce the fine and coarse triangulation on a structured grid. The structure is such that the coarse elements can be formed by an agglomeration of fine elements.

3.1 Two-level Additive Schwarz

Let $\{\Omega_i, i = 1, .., N\}$ be an overlapping covering of $\bar{\Omega}$, such that $\Omega_i \setminus \partial\Omega$ is open for $i \in \{1, .., N\}$. $\Omega_i \setminus \partial\Omega$ is assumed to consist of the interior of a union of fine elements $\tau \in \mathcal{T}_h$. We introduce the notation

$$\mathcal{V}^h(\Omega_i) := \big\{ v_h \in \mathcal{V}^h : \ \text{supp}(v_h) \subset \bar{\Omega}_i \big\}, \tag{19}$$

for the space of piecewise linear vector-valued functions which are supported in $\bar{\Omega}_i$. For $i = 1, .., N$, let R_i be the restriction operator of a function in $\mathcal{V}^h(\bar{\Omega})$ to $\mathcal{V}^h(\Omega_i)$ (more details can be found in [30]). We define the local submatrices of A corresponding to Ω_i by $A_i = R_i A R_i^T$.

Additionally to the local subdomains, we need a coarse triangulation $\mathcal{T}_H$ of $\bar{\Omega}$ into coarse elements. Here, we assume again that each coarse element T consists of a union of fine elements $\tau \in \mathcal{T}_h$ of the fine triangulation. We will construct a coarse basis whose values are determined on the coarse grid points in $\bar{\Omega}$ (excluding coarse DOFs on the Dirichlet boundaries), given by the vertices of the coarse elements in $\mathcal{T}_H$. The coarse space $\mathcal{V}_0^H \subset \mathcal{V}_0^h$ is constructed such that it is a subspace of the vector-field of piecewise linear basis functions on the fine grid. That is, each function $\phi^H \in \mathcal{V}_0^H$ omits a representation w.r.t. the fine scale basis. The *restriction matrix* R_H describes

a mapping from the coarse to the fine space and contains the corresponding coefficients vectors of the coarse basis functions by row. The coarse grid stiffness matrix is then defined as the Galerkin product $A_H := R_H A R_H^T$. With these tools in hand, the action of the two-level additive Schwarz preconditioner is defined implicitly by

$$M_{\mathrm{AS}}^{-1} = R_H^T A_H^{-1} R_H + \sum_{i=1}^{N} R_i^T A_i^{-1} R_i.$$

In the following, we may write A_0 and R_0 instead of A_H and R_H. The following two theorems are basic results in Domain Decomposition theory. Proofs can be found in [30]. Theorem 3.1 also states a reasonable assumption on the choice of the overlapping subdomains.

Theorem 3.1. (Finite Covering) *The set of overlapping subspaces $\Omega_i, i = 1, .., N$ can be colored by $N_C \leq N$ different colours such that if two subspaces Ω_i and Ω_j have the same color, it holds $\Omega_i \cap \Omega_j = \emptyset$. For the smallest possible number N_C, the largest eigenvalue of the two-level preconditioned Schwarz linear system is bounded by*

$$\lambda_{\max}(M_{\mathrm{AS}}^{-1} A) \leq N_C + 1$$

Theorem 3.2. (Stable Decomposition) *Suppose there exists a constant $C_0 \geq 1$, such that for every $v \in \mathcal{V}^h$, there exists a decomposition $u = \sum_{i=0}^{N} u^i$ such that*

$$\sum_{i=0}^{N} a(u^i, u^i) \leq C_0^2 a(u, u).$$

Then, it holds

$$\lambda_{\min}(M_{\mathrm{AS}}^{-1} A) \geq C_0^{-2}.$$

As we can see, the choice of the coarse space has no influence on the largest eigenvalue of the preconditioned system. However, it is crucial for obtaining a small constant C_0 in the estimate of the smallest eigenvalue in Theorem 3.2. We continue with the construction of the structured fine and coarse grid and motivate and define the coarse multiscale basis for linear elasticity in the next sections.

3.2 Fine and Coarse Triangulation

The fine grid: Let the domain Ω be of the form of a 3D cube, i.e. $\bar{\Omega} = [0, L_x] \times [0, L_y] \times [0, L_z] \subset \mathbb{R}^3$ for given $L_x, L_y, L_z > 0$. The fine grid is constructed from an initial voxel structure which is further decomposed into tetrahedral finite elements [28]. More precisely, the set of grid points in $\bar{\Omega}$ is given by

$$\begin{aligned} \bar{\Sigma}_h := \big\{ (x_i, y_j, z_k)^T \mid x_i = ih_x,\, y_j = jh_y,\, z_k = kh_z, \\ i = 0, .., n_x,\, j = 0, .., n_y,\, k = 0, .., n_z \big\} \end{aligned} \tag{20}$$

where $n_x = L_x/h_x,$, $n_y = L_y/h_y$, $n_z = L_z/h_z$. For simplicity, we may assume that $L := L_x = L_y = L_z$ and $h := h_x = h_y = h_z$, and thus $n_h := n_x = n_y = n_z$. That is, the

fine grid can be decomposed into $n_h \times n_h \times n_h$ grid-blocks of size $h \times h \times h$. We denote such a fine grid block by $\square_h^{ijk}$, $1 \leq i, j, k \leq n_h$. The triple (i, j, k) uniquely determines the position of the corresponding block in $\bar{\Omega}$. Each block is further decomposed into 5 tetrahedral elements. The decomposition depends on the position of the specific grid-block. To identify them, we introduce the notation $s^{ijk} := s(\square_h^{ijk}) = i + j + k$. We distinguish between two different decompositions, depending on the value of s^{ijk} mod 2. We follow the numbering of the 8 vertices of a block as given in Figure 1. If s^{ijk} is odd (see Figure 1 (a)), block $\square_h^{ijk}$ is decomposed into 5 tetrahedrons which are defined by the set of their four vertices within each block,

$$\big\{\{1,2,4,6\},\{1,3,4,7\},\{1,5,6,7\},\{4,6,7,8\},\{1,4,6,7\}\big\}.$$

If s^{ijk} is even (see Figure 1 (b)), the decomposition of block $\square_h^{ijk}$ into the tetrahedrons is done such that their vertices are given by

$$\big\{\{1,2,3,5\},\{2,3,4,8\},\{2,5,6,8\},\{3,5,7,8\},\{2,3,5,8\}\big\}.$$

With the given decomposition, a conformal triangulation of Ω into tetrahedral ele-

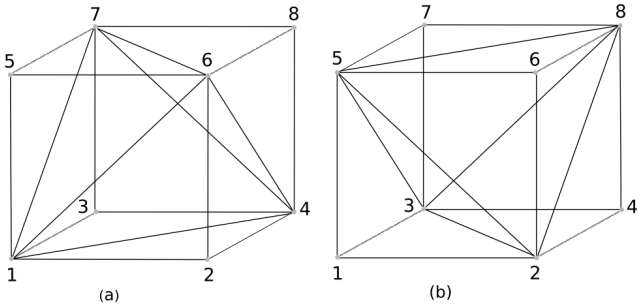

Figure 1: *Decomposition of grid block into 5 tetrahedral elements*

ments is uniquely defined, we denote this partition by $\mathcal{T}_h$. $\mathcal{T}_h$ is referred to as the fine grid triangulation, whereas the coarse grid triangulation, introduced in the following, is denoted by $\mathcal{T}_H$.

Forming coarse elements by agglomeration: The coarse elements $T \in \mathcal{T}_H$ are constructed by an agglomeration of the fine elements. We construct a set of agglomerated elements $\{T\} = \mathcal{T}_H$ such that each $T = \bigcup_{i=1}^{n_T} \tau_i$, $\tau_i \in \mathcal{T}_h$ is a simply connected union of fine grid elements. Thus, for any two $\tau_i, \tau_j \in \mathcal{T}_h$, there exists a connecting path of elements $\{\tau_k\}_k \subset T$ beginning in τ_i and ending in τ_j. Each fine grid element τ should belong to exactly one agglomerated element T. Due to a certain structure of the underlying grid, the agglomeration is done such that the coarse elements have the same tetrahedral form as the fine elements, and automatically form a coarser grid of

equal structure. The table *AE_element* is used to store the fine elements which belong to an agglomerated (coarse) element. Given the fine triangulation $\mathcal{T}_h$ of Ω, the agglomeration process proceeds as follows:

1. Given a fixed coarsening-factor c_f, compute the position of the coarse nodes to decompose the domain Ω into imaginary coarse blocks $\square_H^{ijk}$ of size $H \times H \times H$, where $1 \leq i, j, k \leq n_H \in \mathbb{N}$, $n_H = n_h/c_f$, and $H = c_f h$;

2. Build the *CB_element* table:
   For each $\tau \in \mathcal{T}_h$, measure the position of τ in Ω and assign it to the belonging coarse block $\square_H^{ijk}$;

3. Build the *AE_element* table:
   For each coarse block $\square_H^{ijk} \subset \Omega$ and each $\tau \subset \square_H^{ijk}$ (*CB_element*), measure the position of τ in $\square_H^{ijk}$ and assign it to the belonging coarse tetrahedron;

In step 3 of the agglomeration process, we use again the mapping $s^{ijk} := s(\square_H^{ijk}) = i + j + k$ to identify the coarse tetrahedrons into which a given block is decomposed. This partition automatically defines a set of coarse grid points, given by the vertices of the coarse elements. It remains to be shown that a straightforward decomposition of a coarse block into coarse tetrahedral elements leads to the same result as forming the coarse tetrahedrons by agglomerating fine elements. The proof of this concept will be discussed in more detail in a following report. Having defined the coarse partition $\mathcal{T}_H$ of Ω into tetrahedral elements, we need grid-transfer operators R_H, respectively R_H^T which connect fine and coarse grid. We state the requirements on the interpolation operator and the construction of the coarse multiscale basis in section 5 and proceed with a short background of the multiscale finite element method for scalar elliptic PDEs.

4 From Scalar PDEs to the PDE System

In this section, we shortly review the MsFEM method for scalar elliptic PDEs. More precisely, we show how the linear multiscale finite element basis functions are defined and give the global Galerkin formulation that couples the multiscale basis functions. A detailed and complete introduction into MsFEM methods for scalar PDEs can be found in [9].

4.1 The MsFEM for Scalar Elliptic PDEs

We consider the scalar elliptic PDE

$$-\operatorname{div}(\alpha \nabla u) = f \text{ in } \Omega \tag{21}$$

where $\alpha = \alpha(x)$ is a highly varying field in Ω. For simplicity, we restrict here to homogeneous boundary conditions on $\partial\Omega$. Let $\mathcal{V}_0^{h,\mathrm{s}}(\Omega)$ denote the space of scalar piecewise linear basis functions on the fine triangulation $\mathcal{T}_h$, which vanish on the boundary. We

define the multiscale basis functions on the coarse triangulation $\mathcal{T}_H$ of Ω and construct a multiscale coarse space $\mathcal{V}_0^{H,\mathrm{s}}$ as a subspace of $\mathcal{V}_0^{h,\mathrm{s}}(\Omega)$. We denote the set of coarse grid points in Ω by $\Sigma_H(\Omega)$. It is given by the vertices of the coarse elements $T \in \mathcal{T}_H$ which do not touch the boundary $\partial\Omega$. For each coarse node $x^p \in \Sigma_H$, let

$$S_p = \left\{ T \in \mathcal{T}_H : x^p \in T \right\} \tag{22}$$

be the union of the coarse elements which are attached to the node x^p. We denote the scalar coarse nodal basis function corresponding to x^p by $\phi_p^{\mathrm{lin}} : S_p \to \mathbb{R}$. That is, ϕ_p^{lin} is linear in $T \in \mathcal{T}_H$ and it holds $\phi_p^{\mathrm{lin}}(x^q) = \delta_{pq}, x^q \in \Sigma_H$. For $T \subset S_p$, let $\phi_{p,T}^{\mathrm{ms}} : T \to \mathbb{R}$ be a function which coincides with ϕ_p^{lin} on the boundary ∂T of the coarse element. In the interior of T, let $\phi_{p,T}^{\mathrm{ms}}$ be given by a (discrete) PDE-harmonic extension of the linear boundary data $\phi_p^{\mathrm{lin}} \mid_{\partial T}$. The multiscale basis function $\phi_p^{\mathrm{ms}} : S_p \to \mathbb{R}$ is defined elementwise by

$$\phi_p^{\mathrm{ms}} \mid_T = \begin{cases} \phi_{p,T}^{\mathrm{ms}} & \text{if } x^p \in T \\ 0 & \text{otherwise} \end{cases}$$

To define the fine and coarse stiffness matrix, we introduce the corresponding bilinear form of the PDE given in equation (21) by

$$a^s(u,v) := \int_\Omega \alpha \nabla u \cdot \nabla v \, dx.$$

It defines the entries of the fine stiffness matrix $\tilde{A}^h$ to

$$\tilde{A}_{ij}^h = a^s(\varphi_i, \varphi_j) = \int_\Omega \alpha \nabla \varphi_i \cdot \nabla \varphi_j \, dx.$$

Using the representation of the multiscale basis functions w.r.t the basis on the fine grid, the entries in the coarse stiffness matrix are given by

$$\begin{aligned} \tilde{A}_{pq}^H &= a^s(\phi_p^{\mathrm{ms}}, \phi_q^{\mathrm{ms}}) = \int_\Omega \alpha \nabla \phi_p^{\mathrm{ms}} \cdot \nabla \phi_q^{\mathrm{ms}} \, dx \\ &= \sum_{i,j=1}^{\dim \mathcal{V}_0^{h,\mathrm{s}}} r_{p,i}^s \int_\Omega \alpha \nabla \varphi_i \cdot \nabla \varphi_j \, dx \; r_{q,j}^s. \end{aligned}$$

The coarse stiffness matrix can be computed by the Galerkin product

$$\tilde{A}^H = R_H^s \tilde{A}^h {R_H^s}^T,$$

where the restriction matrix R_H^s contains the coefficient vectors of the multiscale basis functions in terms of the fine-grid basis by rows.

The following condition number estimates show the dependence of the preconditioned system to the mesh parameters [30] and the magnitude of the jumps. It holds

$$\kappa(M_{\mathrm{AS}}^{-1} \tilde{A}^h) \leq C \max_i \sup_{x,y \in \Omega_i} \left(\frac{\alpha(x)}{\alpha(y)} \right) \left(1 + \frac{H}{\delta} \right). \tag{23}$$

Here, H stands for the characteristic mesh size of the coarse triangulation and δ is the smallest overlap diameter of the local subdomains. This estimate is valid for scalar elliptic PDEs using a coarse space which is piecewise linear. However, it may give too pessimistic estimates when other coarse spaces are used. In [12], sharper coefficient explicit condition number bounds for the two-level additive Schwarz method are presented. Their estimates are based on the energy of the coarse basis functions. E.g., assuming that coefficient jumps occur only in the interior of coarse grid elements where the basis functions are locally harmonic, the estimates presented there promise convergence rates independent of variations in the fine mesh parameter h and the material jumps. Therefore, reasonable assumptions on the overlapping subdomains may be required. For the linear elasticity system, such condition number estimates are not yet available.

5 MsFEM for the PDE System of Linear Elasticity

In this section, we extend the scalar MsFEM method as summarized in section (4.1) to the 3D system of linear elasticity. We summarize the main properties of a robust coarse space and state the requirements when applying the multiscale framework to linear elasticity. The motivation is based on the increased kernel of the elasticity operator, which consists of the 6 rigid body modes. In this section, we also give the definition of the multiscale basis and the multiscale coarse space $\mathcal{V}^H = \mathcal{V}^{\text{MS}}$ for linear elasticity, and show some of it's properties. Also, we define the interpolation, respectively the restriction operator and show some details on their construction. We see that the interpolation defined by the multiscale basis functions presented here, satisfies the required properties. We end this section by giving an additional way to define a multiscale coarse space which is spanned only by rigid body rotations.

5.1 Extensions to 3D Linear Elasticity

The proof of the convergence estimates for the scalar elliptic case, given in equation (23), requires a quasi-interpolant (see [5]) for which stability and approximation estimates hold in the semi-norm $|\cdot|_{H^1}$. Using similar arguments and a vector-valued linear coarse space, one can show that a condition number bound $\kappa(M_{\text{AS}}^{-1}A) \leq C\big(1 + \frac{H}{\delta}\big)$ also holds for the system of linear elasticity (see [30]). The additional requirement in the proof is that the coarse space preserves the full kernel of the elasticity operator. However, the constant in the estimate may be very large as it depends on the material coefficients and also on Korn's constant. For any domain $\omega \subset \Omega$, Korn's constant is the smallest constant $C_\omega > 0$, such that

$$|v|^2_{[H^1(\omega)]^3} \leq C_\omega \|\varepsilon(v)\|^2_{[L^2(\omega)]^{3\times 3}}. \tag{24}$$

It strongly depends on the shape of the domain as well as the choice of the boundary conditions. Note that such a constant cannot exist for any $v \in [H^1(\omega)]^3$. It does not hold for functions which characterize a rigid body rotation (see equation (25)). For

any rotation, the right-hand side in equation (24) vanishes while the left one is unequal to zero.

Theorem 3.2 motivates the construction of coarse spaces which allow a nearly $a(\cdot,\cdot)$-orthogonal decomposition for each $v \in \mathcal{V}_h$. Orthogonality can be achieved locally by constructing coarse basis functions which are PDE-harmonic in the interior of coarse elements. This often leads to the argument of constructing coarse basis functions with minimal energy. Such a basis should contain the eigenfunctions corresponding to the smallest eigenvalues of the fine stiffness matrix. These eigenvalues are related to eigenfunctions which are in the kernel of the PDE operator. They occur globally in the computational domain, and locally around any high contrast inclusion.

Requirements of a robust coarse space:

1. The coarse space should approximate well the eigenfunctions corresponding to the smallest eigenvalues of the underlying PDE.

2. The coarse basis functions should be locally supported, to ensure a certain sparsity pattern of the interpolation operator.

The 6 RBMs and their interpolation: In three dimensions, the eigenfunctions in the kernel of the elasticity operator consist of the 6 rigid body modes. They are given by the set

$$\mathcal{RBM}(\bar{\Omega}) = \left\{ a + b \times X : a, b \in \mathbb{R}^3 \right\}. \tag{25}$$

Here, the vector $X = (x_1, x_2, x_3)^T$ denotes the position vector function in $\bar{\Omega}$. As the dependence on the domain $\bar{\Omega}$ is obvious, we may simplify the notation and write $\mathcal{RBM} = \mathcal{RBM}(\bar{\Omega})$ instead. It is easy to verify that for all $u \in [H^1(\Omega)]^3$, it holds $\varepsilon(u) = 0 \Leftrightarrow u \in \mathcal{RBM}$. At least away from the boundary Γ_{D_i}, $i = 1, 2, 3$, where Dirichlet values are prescribed, the interpolation operator should be constructed such that it preserves the six rigid body modes. We describe the construction of the multiscale coarse space and the appropriate interpolation operator in the next section.

5.2 The Multiscale Basis for Linear Elasticity

Let $\mathcal{T}_H$ be the coarse triangulation of Ω in tetrahedral elements, generated from agglomerating fine grid elements as described in the previous section. We construct a MsFEM coarse space $\mathcal{V}^H$ as a subspace of the finite element space $\mathcal{V}^h$ of the piecewise linear vector-valued basis functions (see equation (11)) on the fine triangulation $\mathcal{T}_h$. That is, the coarse space basis functions are represented by their values at the fine-grid DOFs. The coarse grid points in $\bar{\Omega}$ are given by

$$\begin{aligned} \bar{\Sigma}_H := \big\{ (x_i, y_j, z_k)^T \in \mathbb{R}^3, \mid x_i = iH,\, y_j = jH,\, z_k = kH, \\ i, j, k = 0, .., n_H \big\} \end{aligned} \tag{26}$$

where $n_H = c_f h$ and $c_f = H/h \in \mathbb{N}$ denotes the coarsening ratio. To distinguish between a coarse node and the 3 degrees of freedom corresponding to it, we introduce

the set

$$\mathcal{D}^H = \big\{ p^{(m)} \in \mathcal{D}^h, x^p \in \bar{\Sigma}_H, m \in \{1,2,3\} \big\}. \tag{27}$$

That is, for each coarse node $x^p \in \bar{\Sigma}_H$, we denote the m-th coarse degree of freedom, $m \in \{1,2,3\}$, related to this node by $p^{(m)} \in \mathcal{D}^H$. Let

$$S_p = \big\{ T \in \mathcal{T}_H : x^p \in T \big\} \tag{28}$$

be the union of the coarse elements which are attached to the node x^p. We denote the scalar coarse nodal basis function corresponding to x^p by $\phi_p^{\text{lin}} : S_p \to \mathbb{R}$. That is, ϕ_p^{lin} is linear in $T \in \mathcal{T}_h$ and it holds $\phi_p^{\text{lin}}(x^q) = \delta_{pq}, x^q \in \bar{\Sigma}_H$. For $x^p \in \mathbb{R}^3$ and $m \in \{1,2,3\}$ we construct a vector valued multiscale basis function $\phi_{p^{(m)}}^{\text{MS}} : S_p \to \mathbb{R}^3$. The construction is done separately for each element $T \in \mathcal{T}_H$, such that it holds

$$\begin{aligned} \operatorname{div}(\mathrm{C} : \varepsilon(\phi_{p^{(m)}}^{\text{MS}} \mid_T)) &= 0 \text{ in } T, T \subset S_p, & (29) \\ \phi_{p^{(m)}}^{\text{MS}} \mid_T &= \phi_p^{\text{lin}} \mid_T e^m \text{ on } \partial T, T \subset S_p. & (30) \end{aligned}$$

Equation (29) and (30) have to be understood in the sense that they hold for $\phi_{p^{(m)}}^{\text{MS}}$ w.r.t. the discretization given by the fine grid. The vector-field $\phi_{p^{(m)}}^{\text{MS}}$ is homogeneous in $T \subset S_p$. On ∂T, linear boundary conditions are imposed in the m-th component of the vector-field and zero boundary conditions in the components $j \in \{1,2,3\} \setminus \{m\}$. Note that the support S_p of the coarse basis function $\phi_{p^{(m)}}^{\text{MS}}$ is the same for each function $\phi_{p^{(m)}}^{\text{MS}}, m \in \{1,2,3\}$ at the node x^p. Since we prescribe linear boundary conditions on the boundaries of $T \in \mathcal{T}_H$, the multiscale basis functions are continuous along the faces of the coarse elements. That is, it holds $\phi_{p^{(m)}}^{\text{MS}}(x) \mid_{T'} = \phi_{p^{(m)}}^{\text{MS}}(x) \mid_T = \phi_p^{\text{lin}}(x) \mid_T e^m$ for all $x \in \partial T \cap \partial T'$, the corresponding multiscale coarse space is conforming. We define the coarse space $\mathcal{V}^H := \mathcal{V}^{\text{MS}}$ by

$$\mathcal{V}^{\text{MS}} := \operatorname{span}\big\{ \phi_{p^{(m)}}^{\text{MS}}, x^p \in \bar{\Sigma}_H,\, m \in \{1,2,3\} \big\}. \tag{31}$$

In section 5.3 we see that, due to the PDE-harmonic extension of the linear boundary conditions, the space $\mathcal{V}^H$ contains the 6 rigid body modes.

5.3 Properties of the MsFEM Coarse Space

Indeed, assuming constant material coefficients in the PDE, the space $\mathcal{V}^H$ recovers exactly the linear vector valued basis functions on the coarse grid $\mathcal{T}_H$. For the general case of varying coefficients, the following observation shows that the coarse space preserves the 3 translations, separately for each unknown.

Global translations: For $T \in \mathcal{T}_H$, we denote by $\bar{\Sigma}_H(T) := \bar{\Sigma}_H \cap T$ the set of vertices of T. Due to the prescribed linear boundary conditions in equation (30), for each $m \in \{1,2,3\}$ and $T \in \mathcal{T}_H$, it holds

$$\sum_{x^p \in \bar{\Sigma}_H(T)} \phi_{p^{(m)}}^{\text{MS}} = 1_{\bar{\Omega}} e^m \text{ on } \partial T \tag{32}$$

where $1_{\bar{\Omega}}$ stands for the constant function in $\bar{\Omega}$ and e^m is the m-th Cartesian basis vector in $\mathbb{R}^3$. The homogeneous extension of equation (32) to the interior of T by equation (29), together with the uniqueness of the solution, gives

$$\sum_{x^p \in \bar{\Sigma}_H(T)} \phi^{\mathrm{MS}}_{p^{(m)}} = 1_{\bar{\Omega}} e^m \text{ in } T, \tag{33}$$

separately for each coarse element. Furthermore, this local argument can be extended to the global domain and it holds

$$\sum_{x^p \in \bar{\Sigma}_H} \phi^{\mathrm{MS}}_{p^{(m)}} = 1_{\bar{\Omega}} e^m \text{ in } \bar{\Omega}.$$

Thus, the 3 translations are contained in the coarse space $\mathcal{V}^H$, separately for each unknown $m \in \{1,2,3\}$.

Global rotations: Next, we show that the introduced space $\mathcal{V}^H$ contains also the 3 rigid body rotations.

Lemma 5.1. *The six rigid body modes are contained in the space $\mathcal{V}^H$. That is, it holds*

$$\mathcal{RBM} \subset \mathcal{V}^H.$$

Proof: We have to show that $e^m \times x \in \mathcal{V}^H$, $m \in \{1,2,3\}$. Here, we do not distinguish in our notation between a point $x \in \mathbb{R}^3$ and the identity mapping $x : \bar{\Omega} \to \mathbb{R}^3$, $x \mapsto x$, assuming that this should not lead to any confusion. For each $x^q \in \bar{\Sigma}_H$, $r \in \{1,2,3\}$, we define the vector

$$\beta^{q(r)} := e^r \times x^q \in \mathbb{R}^3,$$

and denote its components by $\beta^{q(r)}_s := \beta^{q(r)} \cdot e^s \in \mathbb{R}$. We have $x = \sum_{x^q \in \bar{\Sigma}_H} x^q \phi^{\mathrm{lin}}_q(x)$ in $\bar{\Omega}$. In what follows, we first assume $x \in \partial T, T \in \mathcal{T}_H$. It holds

$$\begin{aligned} e^m \times x &= \sum_{x^q \in \bar{\Sigma}_H} (e^m \times x^q) \phi^{\mathrm{lin}}_q(x) \quad \text{on } \partial T \\ &= \sum_{x^q \in \bar{\Sigma}_H} \sum_{s=1}^{3} (e^m \times x^q) \cdot e^s \, \phi^{\mathrm{lin}}_q(x) \, e^s \quad \text{on } \partial T \\ &= \sum_{x^q \in \bar{\Sigma}_H} \sum_{s=1}^{3} \beta^{q(m)}_s \phi^{\mathrm{MS}}_{q^{(s)}}(x) \quad \text{on } \partial T. \end{aligned}$$

Thus, along the boundaries of the coarse elements $T \in \mathcal{T}_H$, we can represent $e^m \times x$ as a linear combination of functions in $\mathcal{V}^H$. With the argument which we used to validate equation (33), together with the uniqueness of the solution, we have

$$e^m \times x = \sum_{x^q \in \bar{\Sigma}_H} \sum_{s=1}^{3} \beta^{q(m)}_s \phi^{\mathrm{MS}}_{q^{(s)}}(x) \text{ in } T,$$

locally for each $T \in \mathcal{T}_H$ and thus, also globally in $\bar{\Omega}$. The uniqueness argument holds here since, by equation (25), the vector-field $e^m \times x$ is in the kernel of the elasticity operator and thus, it is a solution of $\operatorname{div}(\mathrm{C} : \varepsilon) = 0$. □

Note that we concluded that from $\sum_q \phi^{\mathrm{MS}}_{q^{(m)}} \in \mathcal{V}^H$, $m \in \{1,2,3\}$, it follows $\sum_q \phi^{\mathrm{MS}}_{q^{(m)}} \times e^m \in \mathcal{V}^H$. Indeed, this only holds for the sum of the basis functions, but not separately for each basis function. In general, we have $\phi \in \mathcal{V}^H \not\Rightarrow \phi \times e^m \in \mathcal{V}^H$. This characterizes the main differences between the introduced space $\mathcal{V}^H$ and the space $\mathcal{V}^H_{\mathrm{Rot}}$ which will be introduced in section 5.6.

5.4 The MsFEM Interpolation Operator:

In the following, we form the interpolation operator which is implicitely defined by the multiscale coarse basis. Let us first summarize some notations. The number of grid points in $\bar{\Omega}$ on the fine grid is denoted by n_p, the number of grid points on the coarse grid is denoted by N_p. To each grid point, fine or coarse, we associate a vector-field $u = (u_1, u_2, u_3)^T : \bar{\Omega} \to \mathbb{R}^3$ of displacements. We denote the corresponding components $u_i, i = 1,2,3$ of the vector-field by *unknowns*. The unknowns are defined on the same grid-hierarchy. The number of fine and coarse degrees of freedom on the fine and coarse triangulation (in $\bar{\Omega}$) is given by $n_d = 3n_p$, $N_d = 3N_p$, respectively. Furthermore, for $\beta \in \{h, H\}$, the set $\mathcal{D}^\beta = \mathcal{D}^\beta(\bar{\Omega})$ denotes the index set of fine ($\beta = h$), respectively coarse ($\beta = H$) degrees of freedom of $\mathcal{V}^\beta$. For any subset $W \subset \bar{\Omega}$, let $\mathcal{D}^\beta(W) \subset \mathcal{D}^\beta(\bar{\Omega})$ be the restriction of $\mathcal{D}^\beta$ to the local set of degrees of freedom in W, given in a local numbering. To keep the notation with indices simpler for the reader, we use the following convention. To indicate fine degrees of freedom in $\mathcal{D}^h$, we use either index i or j combined with an upper script $k, l \in \{1,2,3\}$, while the index p or q with upper script $m, r \in \{1,2,3\}$ is used to indicate a coarse degree of freedom in $\mathcal{D}^H$. We use the fine scale representation of a coarse basis function $\phi^{\mathrm{MS}}_{p^{(m)}}$ to define the interpolation operator, respectively the restriction operator. Each multiscale basis function omits the representation

$$\phi^{\mathrm{MS}}_{p^{(m)}} = \sum_{k=1}^{3} \sum_{i=1}^{n_p} \bar{r}_{p^{(m)}, i^{(k)}} \varphi_i e^k. \tag{34}$$

This representation defines the matrix $\bar{R} \in \mathbb{R}^{N_d \times n_d}$ which contains the coefficient vectors, representing a coarse basis function in terms of the fine scale basis, by rows. Note that $\bar{R}$ does not define the final restriction operator used in the additive Schwarz setting. Assuming a numbering of the degrees of freedom by unknowns, the matrix $\bar{R}$ admits the block-decomposition

$$\bar{R} = \left(\bar{R}^{IJ}\right)_{I,J=1}^{3} \tag{35}$$

where $\bar{R}_{IJ} \in \mathbb{R}^{N_p \times n_p}$. Each block satisfies

$$\sum_{p=1}^{N_p} \bar{R}^{IJ}_{p,j} = \delta_{IJ} \quad \forall j \in \{1, .., n_p\}.$$

That is, the column sum of the diagonal-blocks is one, while the off-diagonals have column-sum zero. Note that, this is only true for the sum of the columns of each block. In general, this is not true for the components itself. For $I \neq J$, we have $\bar{R}^{IJ}_{p,j} = 0$ for all $p \in \{1, .., N_p\}$ and $j \in \{1, .., n_p\}$ if and only if the underlying material is homogeneous. In this case, where no coefficient jumps occur, the multiscale basis functions exactly recover the vector-valued piecewise linear basis functions on the coarse grid, separately for each unknown. By construction, each row of the matrix $\bar{R}$ contains the fine-scale representation of a basis function of $\mathcal{V}^H$. The restriction operator R_H, which we use in the Additive Schwarz algorithm is then constructed as a submatrix of $\bar{R}$, which contains only the rows corresponding to coarse basis functions of $\mathcal{V}^H_0$. Thus, it contains the rows related to coarse basis functions which vanish on the global Dirichlet boundaries Γ_{D_i}, $i = 1, 2, 3$. Denoting the entries of R_H by $(r_{p',j'})_{p',j'}$, we define

$$r_{p',j'} = \bar{R}_{p',j'}, \;\; p' \in \mathcal{D}^H(\Omega^*), \;\; j' \in \mathcal{D}^h(\bar{\Omega}),$$

where $\mathcal{D}^H(\Omega^*)$, $\Omega^* := \bar{\Omega} \backslash (\cup^i \Gamma_{D_i})$ denotes the coarse interior degrees of freedom in Ω^*. The matrix representing the interpolation from the coarse space $\mathcal{V}^H_0$ to the fine space $\mathcal{V}^h_0$ is simply given by the transposed, R^T_H. The entries in the corresponding coarse stiffness matrix are

$$\begin{aligned} A^H_{p^{(m)} q^{(r)}} &= \int_\Omega \tilde{\varepsilon}(\phi^{\mathrm{MS}}_{p^{(m)}})^T \, \tilde{\mathrm{C}} \, \tilde{\varepsilon}(\phi^{\mathrm{MS}}_{q^{(r)}}) \, dx \\ &= \sum_{k,l=1}^{3} \sum_{i,j=1}^{n_h} r_{p^{(m)}, i^{(k)}} \int_\Omega \tilde{\varepsilon}(\varphi_i e^k)^T \tilde{\mathrm{C}} \tilde{\varepsilon}(\varphi_j e^l) \, dx \, r_{q^{(r)}, j^{(l)}} \end{aligned} \tag{36}$$

and the coarse stiffness matrix can be computed by the Galerkin product $A^H = R_H A R^T_H$.

5.5 Construction of the MsFEM Basis Functions

The element-wise construction: Let $T \in \mathcal{T}_H$ be a coarse tetrahedral element, let x_p be a vertex of T and let $m \in \{1, 2, 3\}$. By construction, $T = \cup \{\tau_i\}_{i=1}^{n_T}$ consists of a union of fine elements in $\mathcal{T}_h$. Recall the space $\mathcal{V}^h$ of piecewise linear vector-valued nodal functions on $\mathcal{T}_h$ in $\bar{\Omega}$. Let $\mathcal{V}^h(T) = \{\varphi \in \mathcal{V}^h : \; \mathrm{supp}(\varphi) \subset T\}$ be the set of functions in $\mathcal{V}^h$ which are supported in T and let $\mathcal{V}^h_{|T} := \{\varphi|_T : \; \varphi \in \mathcal{V}^h\}$ denote the restriction of functions in $\mathcal{V}^h$ to T. Note that T is a closed subset of $\bar{\Omega}$ and $\mathcal{V}^h_{|T}$ contains also the functions which do not vanish on ∂T. We denote the restriction of the bilinear form defined in equation (9) to a coarse element T by $a_T(\,\cdot\,,\,\cdot\,) : \mathcal{V}^h_{|T} \times \mathcal{V}^h_{|T} \to \mathbb{R}$. It is given by $a_T(u, v) := \int_T (\mathrm{C} : \varepsilon(u)) : \varepsilon(v) \, dx$. Thus, from equation (29) and (30), we obtain the local linear system $A_T \Phi^{p^{(m)}}_T = \mathbf{f}^{p^{(m)}}_T$. It is formed following the construction provided in section 2.3, with $\bar{\Omega}$ replaced by T, and Γ_{D_i}, $i = 1, 2, 3$ replaced by ∂T. As boundary conditions, $u = \varphi^p_{\mathrm{lin}} \mathbf{e}_m$ on ∂T is imposed. The solution $\Phi^{p^{(m)}}_T$ of the linear system defines the solution to the problem in equation (29) and (30), discretized on the space $\mathcal{V}^h_{|T}$. It is given by $\phi^{\mathrm{MS}}_{p^{(m)}|T} = \sum_{j^{(k)} \in \mathcal{D}^h_{|T}(\bar{\Omega})} \Phi^{p^{(m)}}_{T, j^{(k)}} \phi_{j^{(k)}|T}$. Here, $\mathcal{D}^h_{|T}(\bar{\Omega})$ denotes

the restriction of the global degrees of freedom $\mathcal{D}^h(\bar{\Omega})$ to the element T. Note that the table *AE_element* formed in the element agglomeration process described in section 3.2 provides the required information of the fine elements contained in $T = \cup\{\tau_i\}_{i=1}^{n_T}$.

Construction of the multiscale basis: Summarized, the procedure for the construction of the MsFEM basis is as follows:

1. For each coarse element $T \in \mathcal{T}_H$, the following applies
   - for each vertex x^p of T and $m \in \{1,2,3\}$, compute the solution $\phi^{\mathrm{MS}}_{p^{(m)}}|_T$ of the PDE given in equation (29) and (30). Therefore, follow the procedure described above.
2. For each coarse grid-point $x^p \in \bar{\Sigma}_H$ and $m \in \{1,2,3\}$, the following applies
   - assemble $\phi^{\mathrm{MS}}_{p^{(m)}} : S_p \to \mathbb{R}^3$ from the computed vector-fields $\phi^{\mathrm{MS}}_{p^{(m)}}|_T : T \to \mathbb{R}^3$ for which $T \subset S_p$ shares the vertex x^p (see (28)). Therefore, assemble $\Phi^{p^{(m)}} \in \mathbb{R}^{n_d}$ by

$$\Phi^{p^{(m)}}_{j^{(k)}} = \begin{cases} \Phi^{p^{(m)}}_{T,j^{(k)}} & \text{if } x^j \in \Sigma_h \cap T, T \subset S_p \\ 0 & \text{otherwise.} \end{cases}$$

     The given vector defines the rows in the matrix $\bar{R}$ as given in equation (34). Note that since the basis function $\phi^{\mathrm{MS}}_{p^{(m)}}$ is continuous along the element boundaries, the vector $\Phi^{p^{(m)}}$ is well-defined.

5.6 An Additional Coarse Space Formed by Rigid Body Rotations

We have seen that the multiscale coarse space $\mathcal{V}^H$, introduced in section 5.2, contains the full kernel of the elasticity operator. In this section, we give some remarks on an alternative construction of a coarse space $\mathcal{V}^H_{\mathrm{Rot}}$, which spans the three rigid body rotations. The construction is similar to that of $\mathcal{V}^H$, but different boundary conditions are applied for the basis functions. With the definitions as in section 5.2, for each $x^p \in \bar{\Sigma}_H$, $T \subset S_p$, and $m \in \{1,2,3\}$, we define $\phi^{\mathrm{R}}_{p^{(m)}} : S_p \to \mathbb{R}^3$ by

$$\begin{aligned} \mathrm{div}(\mathrm{C} : \varepsilon(\phi^{\mathrm{R}}_{p^{(m)}}\,|_T)) &= 0 \text{ in } T,\ T \subset S_p, & (37)\\ \phi^{\mathrm{R}}_{p^{(m)}}(x)\,|_T &= \phi^{\mathrm{lin}}_p(x)\,|_T\ e^m \times x \text{ on } \partial T,\ T \subset S_p. & (38) \end{aligned}$$

Again, equation (37) and (38) have to be understood in the sense that they hold for $\phi^{\mathrm{R}}_{p^{(m)}}$ w.r.t. the discretization given by the fine grid. The vector-field $\phi^{\mathrm{R}}_{p^{(m)}}$ is homogeneous in $T \subset S_p$. On ∂T, the boundary conditions are imposed such that they preserve the rigid body rotation around the m-th axis, multiplied with a linear partition of unity function. The support S_p of the coarse basis function $\phi^{\mathrm{R}}_{p^{(m)}}$ coincides for each $m \in \{1,2,3\}$. Due to the prescribed boundary conditions along the faces of the coarse elements, the corresponding coarse space

$$\mathcal{V}^H_{\mathrm{Rot}} := \mathrm{span}\big\{\phi^{\mathrm{R}}_{p^{(m)}}, x^p \in \bar{\Sigma}_H,\, m \in \{1,2,3\}\big\} \quad (39)$$

is conforming. In the following we show that the space $\mathcal{V}_{\text{Rot}}^H$ contains the 3 rigid body rotations, locally as well as globally in $\bar{\Omega}$. Due to the prescribed boundary conditions in equation (38), we have for $m \in \{1, 2, 3\}$ and $T \in \mathcal{T}_H$,

$$\sum_{x^p \in \bar{\Sigma}_H(T)} \phi_{p^{(m)}}^{\text{R}}(x) = 1_{\bar{\Omega}} e^m \times x \text{ on } \partial T \tag{40}$$

where, again, $1_{\bar{\Omega}}$ stands for the constant function in $\bar{\Omega}$ and e^m is the m-th Cartesian basis vector in $\mathbb{R}^3$. With the same argument as we used in equation (33), here applied to equation (37), and the uniqueness of the solution, we have

$$\sum_{x^p \in \bar{\Sigma}_H(T)} \phi_{p^{(m)}}^{\text{R}}(x) = 1_{\bar{\Omega}} e^m \times x \text{ in } T. \tag{41}$$

The uniqueness argument holds here since, by equation (25), the vector-field $e^m \times x$ is in the kernel of the elasticity operator and thus, it is a solution of $\text{div}(\text{C} : \varepsilon) = 0$. Again, we extend the local argument to a global one and get

$$\sum_{x^p \in \bar{\Sigma}_H} \phi_{p^{(m)}}^{\text{R}}(x) = 1_{\bar{\Omega}} e^m \times x \text{ in } \Omega.$$

This shows that the 3 rotations are contained in the coarse space $\mathcal{V}_{\text{Rot}}^H$.

The space $\mathcal{V}_{\text{Rot}}^H$: We have seen in section 5.3, due to the linear boundary conditions, a straightforward extension of the scalar (linear) multiscale finite element approach to elasticity leads to a coarse space $\mathcal{V}^H$ which exactly contains the six rigid body motions. However, if the material coefficients vary strongly near the boundary of coarse elements, oscillatory boundary conditions as suggested in [14] for scalar elliptic PDEs may be more appropriate. In the scalar case, oscillatory boundary conditions are extracted by solving the harmonic PDE restricted to the edges ($1D$) and faces ($2D$) of coarse elements. To solve the 1D problem on the edges, the Dirichlet conditions are chosen to be 1 at one endpoint, and 0 at the other. In the scalar case, this procedure of extracting boundary values by solving harmonic problems ensures that constants are preserved along the edges, the faces, and in the interior of coarse elements. However, in linear elasticity, rotations do not occur in 1D problems and thus, the coarse space might not contain all the rigid body rotations anymore, when oscillatory boundary conditions are applied. In applications where the prescribed boundary conditions do not allow all the six rigid body motions to be contained in the coarse space, the space $\mathcal{V}_{\text{Rot}}^H$ gives a possibility of how to extend the coarse space, but special attention has to be paid to ensure that the extension is done such that it does not lead to linear dependencies of the coarse space.

6 Numerical Experiments

In this section, we give a series of examples involving binary media, showing the performance of our multiscale preconditioner under variations of the mesh parameters

as well as the material coefficients. In addition to that, we measure the approximation error of the multiscale coarse space to a fine scale solution. In each experiment, we compare the multiscale coarse space with a standard linear coarse space. We perform our simulations on the domain $\bar{\Omega} = [0,1] \times [0,1] \times [0,L], L > 0$, with fine and coarse mesh as introduced in section 3.2. In our experiments, we consider two variants of heterogeneous media. First, we assume that the discontinuities are isolated, such that the material jumps occur only in the interior of coarse elements. Figure 2 shows such a binary medium with one inclusion inside each coarse tetrahedral element. In a

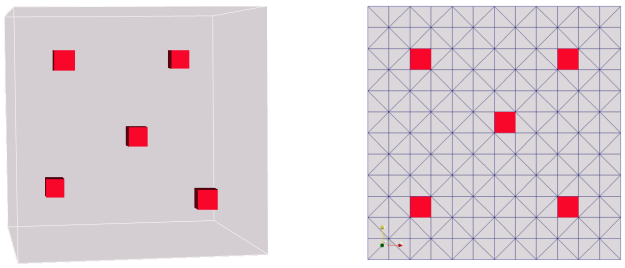

Figure 2: *Medium 1: binary composite; matrix material (grey) and* 1x1x1 *inclusions (red); discretization in* 12x12x12 *voxels; each voxel is decomposed in* 5 *tetrahedrons; 3D view (left) and 2D projection with fine mesh, showing the position of the inclusions (right);*

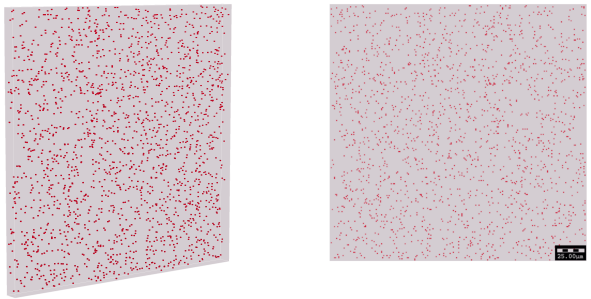

Figure 3: *Medium 2: binary medium consiting of* 240x240x12 *voxels; matrix material (grey) and* 1x1x1 *inclusions (red) identically distributed; 3D view (left) and 2D projection showing the position of the inclusions (right);*

second set of experiments, we do not impose any restriction on the position of the small inclusions. More precisely, we generate a binary medium whose inclusions are identically distributed. An example of such a medium is given in Figure 3.

In the following, we refer to the binary medium where inclusions are isolated in the interior of coarse elements as Medium 1, while the medium with the random distribution of the inclusions is referred to as Medium 2. For each media, the Young's modulus E as well as Poisson ratio ν for matrix material and inclusions are given in Table 1. The contrast $E_c := E_{inc}/E_{mat}$ may vary over several orders of magnitude.

Young's modulus	Poisson ratio
$E_{\text{mat}} = 1$ MPa	$\nu_{\text{mat}} = 0.2$
$E_{\text{inc}} = E_c E_{\text{mat}}$	$\nu_{\text{inc}} = 0.2$

Table 1: *Young's Modulus and Poisson ratio of matrix material and inclusions*

6.1 Coarse Space Robustness

Let $\Omega_p, p \in 1, .., N$ be given by the set of coarse elements which are attached to node $x^p \in \bar{\Sigma}_H$. Then, $\{\Omega_p, p = 1, .., N\}$ defines an overlapping covering of $\bar{\Omega}$ into local subdomains, often referred to as a *generous overlap*. We perform tests observing the performance of the two-level Additive Schwarz preconditioner using linear and multiscale coarsening. We show condition numbers as well as iteration numbers of the Preconditioned Conjugate Gradient (PCG) algorithm. The stopping criterion is to reduce the preconditioned initial residual by 6 orders of magnitude, i.e. $\|r\|_{M_{AS}^{-1}} \leq 10^{-6}\|r_0\|_{M_{AS}^{-1}}$. The estimated condition numbers of $\kappa(M_{AS}^{-1}A)$ are computed based on the three term recurrence which is implicitely formed by the coefficients within the PCG algorithm (c.f. [26]).

In a first experiment (1), we test the robustness of the method on Medium 1 for fixed mesh parameters under the variation of the contrast E_c. The Tables 2 and 3 show the corresponding condition numbers and iteration numbers having stiff ($E_c > 1$) and soft ($E_c < 1$) inclusions. In the former case, robustness is achieved only for the MsFEM coarse space, while linear coarsening leads to non-uniform convergence results. In

	Linear		MsFEM	
E_c	n_{it}	$\kappa(M_{AS}^{-1}A)$	n_{it}	$\kappa(M_{AS}^{-1}A)$
10^0	13	4.4	13	4.4
10^3	21	18.7	13	4.4
10^6	25	109.0	13	4.4
10^9	25	109.0	13	4.4

Table 2: *Iteration numbers n_{it} and condition numbers $\kappa(M_{AS}^{-1}A)$ for Experiment 1; geometry: $1/h$ x $1/h$ x H/h, $h = 1/240$, $H = 12h$; linear and multiscale coarsening for different contrasts $E_c \geq 1$;*

	Linear		MsFEM	
E_c	n_{it}	$\kappa(M_{AS}^{-1}A)$	n_{it}	$\kappa(M_{AS}^{-1}A)$
10^{-0}	13	4.4	13	4.4
10^{-3}	13	4.4	13	4.4
10^{-6}	13	4.4	13	4.4
10^{-9}	13	4.4	13	4.4

Table 3: *Iteration numbers n_{it} and condition numbers $\kappa(M_{AS}^{-1}A)$ for Experiment 1; geometry: $1/h$ x $1/h$ x H/h, $h = 1/240$, $H = 12h$; linear and multiscale coarsening for different contrasts $E_c \leq 1$;*

	Linear		MsFEM	
h	n_{it}	$\kappa(M_{AS}^{-1}A)$	n_{it}	$\kappa(M_{AS}^{-1}A)$
1/60	14	7.9	13	4.4
1/120	17	28.1	13	4.4
1/180	21	61.8	13	4.4
1/240	25	109.0	13	4.4

Table 4: *Iteration numbers n_{it} and condition numbers $\kappa(M_{AS}^{-1}A)$ for Experiment 2; geometry: $1/h$ x $1/h$ x H/h; $H = 12h$; linear and multiscale coarsening for different h; contrast: $E_c = 10^6$;*

the later case, both coarse spaces are bounded in energy, an upper natural bound is evidently given for $E_c = 1$. Linear coarse space and multiscale coarse space perform equally well.

In Experiment 2, performed on Medium 1, we measure the condition numbers and iteration numbers under variation of the mesh parameters, while the coefficients of the PDE remain fixed. We observe similar results as in Experiment 1. Table 4 shows iteration and condition numbers for linear and multiscale coarsening. For the linear coarse space, the condition number shows a linear dependence on the number of subdomains, while the condition number for multiscale coarsening is uniformly bounded.

To summarize, Experiment 1 and 2 show mesh and coefficient independent iteration and condition numbers for the multiscale coarse space when the inclusions are isolated. In a second part, we test the performance of the method when the small inclusions are allowed to touch coarse element boundaries. More precisely, we perform the same experiments again and replace Medium 1 by Medium 2. We denote them by Experiment 3 and Experiment 4. As we already know, we cannot expect coefficient independent convergence rates when the inclusions in the binary medium are such that they cross coarse element boundaries. This is what we see in the Tables 5 and 6 for Experiment 3: For fixed mesh parameters under the variation of the contrast E_c, they show the corresponding condition numbers and iteration numbers having stiff ($E_c > 1$)

and soft ($E_c < 1$) inclusions. Robustness is only achieved in the later case where soft inclusions are considered. For stiff inclusions, both coarsening strategies lead to iteration numbers and condition numbers which strongly depend on the contrast in the medium. We observe that in comparison with linear coarsening, the multiscale coarse space performs only slightly better.

	Linear		MsFEM	
E_c	n_{it}	$\kappa(M_{AS}^{-1}A)$	n_{it}	$\kappa(M_{AS}^{-1}A)$
10^0	13	4.4	13	4.4
10^3	27	19.3	18	8.4
10^6	66	414	78	373
10^9	68	427	75	465

Table 5: *Iteration numbers n_{it} and condition numbers $\kappa(M_{AS}^{-1}A)$ for Experiment 3; geometry: $1/h$ x $1/h$ x H/h, $h = 1/240$, $H = 12h$; linear and multiscale coarsening for different contrasts $E_c \geq 1$;*

	Linear		MsFEM	
E_c	n_{it}	$\kappa(M_{AS}^{-1}A)$	n_{it}	$\kappa(M_{AS}^{-1}A)$
10^{-0}	13	4.4	13	4.4
10^{-3}	13	4.4	13	4.4
10^{-6}	13	4.4	13	4.4
10^{-9}	13	4.4	13	4.4

Table 6: *Iteration numbers n_{it} and condition numbers $\kappa(M_{AS}^{-1}A)$ for Experiment 3; geometry: $1/h$ x $1/h$ x H/h, $h = 1/240$, $H = 12h$; linear and multiscale coarsening for different contrasts $E_c \leq 1$;*

In Experiment 4, we measure the condition numbers and iteration numbers under variation of the mesh parameters for Medium 2. The PDE coefficients remain fixed. The results agree with the observations in Experiment 3. Table 7 shows iteration and condition numbers for linear and multiscale coarsening. Again, for each coarse space, iteration numbers as well as condition numbers grow with the number of subdomains. The multiscale coarse space does not perform noticeably better than the linear coarse space.

6.2 Coarse Space Approximation

In a second set of experiments, we test the approximation properties of the multiscale coarse space. The domain $\bar{\Omega} = [0,1] \times [0,1] \times [0,L]$ contains again a binary medium with small inclusions. Again, we distinguish between Medium 1 (Figure 2: inclusions

	Linear		MsFEM	
h	n_{it}	$\kappa(M_{AS}^{-1}A)$	n_{it}	$\kappa(M_{AS}^{-1}A)$
1/60	26	39.2	27	37.7
1/120	48	154	43	109
1/180	52	261	62	230
1/240	66	414	78	373

Table 7: *Iteration numbers n_{it} and condition numbers $\kappa(M_{AS}^{-1}A)$ for Experiment 4; geometry: $1/h$ x $1/h$ x H/h; $H = 12h$; linear and multiscale coarsening for different h; contrast: $E_c = 10^6$;*

in the interior of each coarse element) and Medium 2 (Figure 3: randomly distributed inclusions). We solve the linear system $-\text{div}\sigma(u) = f$ in $\Omega \setminus \Gamma_D$ with a constant volume force $f = (1, 1, 0)^T$ in the x- and y-component. Zero Dirichlet and Neumann boundary conditions are applied on the boundary $\partial\Omega$. Dirichlet conditions in the first unknown are given on $\Gamma_{D_1} = \{(x, y, z)^T \in \partial\Omega : x = 0, x = 1\}$, in the second unknown on $\Gamma_{D_2} = \{(x, y, z)^T \in \partial\Omega : y = 0, y = 1\}$, and in the third unknown on $\Gamma_{D_3} = \{(x, y, z)^T \in \partial\Omega : z = 0, z = L\}$.

Let u_h denote the approximate solution on a fine mesh $\mathcal{T}_h$. With the bilinear form defined in equation (10) and the space $\mathcal{V}_0^h$ of piecewise linear vector-valued basis functions as defined in equation (12), it holds $a(u_h, v_h) = F(v_h)\ \forall v_h \in \mathcal{V}_0^h$. This formulation leads to the linear system $A\mathbf{u_h} = \mathbf{f_h}$. Let $\mathcal{V}_0^H$ be the space of multiscale finite element functions on the coarse triangulation $\mathcal{T}_H$ which vanish on the Dirichlet boundary Γ_D. The multiscale finite element solution is given by $u_H^{MS} \in \mathcal{V}_0^H$, such that $a(u_H^{MS}, v_H^{MS}) = F(v_H^{MS})\ \forall v_H^{MS} \in \mathcal{V}_0^H$. Using the fine-scale representation of a multiscale basis function as defined in equation (34), the equivalent linear system reads $A_H\mathbf{u}_H = \mathbf{f}_H$. Here, $A_H = R_H A R_H^T$ is the coarse stiffness matrix defined in equation (36), $\mathbf{f}_H = R\mathbf{f}_h$ and $\mathbf{u}_H^{MS} = R^T\mathbf{u}_H$ is the vector whose entries define the fine-scale representation of u_H^{MS} in terms of the basis of $\mathcal{V}_0^h$.

For fixed mesh parameters h and H, under the variation of the contrast E_c, the Tables 8 and 9 show the relative approximation errors $\|\mathbf{u}_h - \mathbf{u}_H^c\|$ in l_2 and in the "energy"-norm for linear (c=LIN) and multiscale (c=MS) coarse space for Medium 1 and Medium 2, respectively. The fine solution $\mathbf{u}_h$ is computed approximately within the PCG algorithm by reducing the initial preconditioned residual by 12 orders of magnitude. The coarse solution $\mathbf{u}_H^c$ is computed exactly by a sparse direct solve of the coarse linear system. For Medium 1, the multiscale coarse space gives stable approximation errors, only slightly varying with the contrast. This is not the case anymore for the linear coarse space. For $E_c \gg 1$, the fine-scale solution is contained in a space which is nearly A-orthogonal to the space spanned by the linear coarse basis functions. Note that this is in agreement with the results presented in Table 4, where the condition number grows almost linearly with the number of subdomains. For $E_c \to \infty$, the coarse space does not correct the error anymore, the two-level method tends to perform

E_c	$\frac{\|\mathbf{u}_h-\mathbf{u}_H^c\|_{l_2}}{\|\mathbf{u}_h\|_{l_2}}$ Linear	MsFEM	$\frac{\|\mathbf{u}_h-\mathbf{u}_H^c\|_A}{\|\mathbf{u}_h\|_A}$ Linear	MsFEM
10^{-9}	$8.63 \cdot 10^{-3}$	$8.11 \cdot 10^{-3}$	$8.92 \cdot 10^{-2}$	$8.54 \cdot 10^{-2}$
10^{-6}	$8.63 \cdot 10^{-3}$	$8.11 \cdot 10^{-3}$	$8.92 \cdot 10^{-2}$	$8.54 \cdot 10^{-2}$
10^{-3}	$8.63 \cdot 10^{-3}$	$8.11 \cdot 10^{-3}$	$8.91 \cdot 10^{-2}$	$8.54 \cdot 10^{-2}$
10^{0}	$8.09 \cdot 10^{-3}$	$8.09 \cdot 10^{-3}$	$8.53 \cdot 10^{-2}$	$8.53 \cdot 10^{-2}$
10^{3}	$7.39 \cdot 10^{-1}$	$9.42 \cdot 10^{-3}$	$8.60 \cdot 10^{-1}$	$9.44 \cdot 10^{-2}$
10^{6}	$9.97 \cdot 10^{-1}$	$9.44 \cdot 10^{-3}$	$9.99 \cdot 10^{-1}$	$9.45 \cdot 10^{-2}$
10^{9}	$9.97 \cdot 10^{-1}$	$9.44 \cdot 10^{-3}$	$9.99 \cdot 10^{-1}$	$9.45 \cdot 10^{-2}$

Table 8: *Approximation of fine-scale solution by linear and MsFEM coarse space for Medium 1; geometry:* $1/h$ *x* $1/h$ *x* H/h, $h = 1/120$, $H = 12h$;

as the one-level method. Considering Medium 2, both coarse spaces only show a weak approximation of the fine-scale solution for high contrasts $E_c \gg 1$. We can summarize

E_c	$\frac{\|\mathbf{u}_h-\mathbf{u}_H^c\|_{l_2}}{\|\mathbf{u}_h\|_{l_2}}$ Linear	MsFEM	$\frac{\|\mathbf{u}_h-\mathbf{u}_H^c\|_A}{\|\mathbf{u}_h\|_A}$ Linear	MsFEM
10^{-9}	$8.60 \cdot 10^{-3}$	$8.25 \cdot 10^{-3}$	$8.90 \cdot 10^{-2}$	$8.65 \cdot 10^{-2}$
10^{-6}	$8.60 \cdot 10^{-3}$	$8.25 \cdot 10^{-3}$	$8.90 \cdot 10^{-2}$	$8.65 \cdot 10^{-2}$
10^{-3}	$8.60 \cdot 10^{-3}$	$8.25 \cdot 10^{-3}$	$8.90 \cdot 10^{-2}$	$8.65 \cdot 10^{-2}$
10^{0}	$8.09 \cdot 10^{-3}$	$8.09 \cdot 10^{-3}$	$8.53 \cdot 10^{-2}$	$8.53 \cdot 10^{-2}$
10^{3}	$7.01 \cdot 10^{-1}$	$3.12 \cdot 10^{-1}$	$8.37 \cdot 10^{-1}$	$5.58 \cdot 10^{-1}$
10^{6}	$9.99 \cdot 10^{-1}$	$9.95 \cdot 10^{-1}$	$1.00 \cdot 10^{-0}$	$9.97 \cdot 10^{-1}$
10^{9}	$1.00 \cdot 10^{-0}$	$9.99 \cdot 10^{-1}$	$1.00 \cdot 10^{-0}$	$9.99 \cdot 10^{-1}$

Table 9: *Approximation of fine-scale solution by linear and MsFEM coarse space for Medium 2; geometry:* $1/h$ *x* $1/h$ *x* H/h, $h = 1/120$, $H = 12h$;

the obtained results as follows. Assuming that the discontinuities are isolated in the interior of coarse elements, the energy of a multiscale basis function is bounded independently of the Young's modulus of the inclusions. Our experiments show uniform condition number bounds w.r.t. both, coefficient variations in the Young's modulus and the mesh size. When the distribution of the inclusions is such that they cross coarse element boundaries, the linear multiscale basis function cannot capture the smallest eigenvalues associated to those inclusions which touch the coarse element boundary. The energy of the basis function strongly depends on the Young's modulus of the inclusion. As the experiments show, no uniform iteration number and condition

number bounds are achieved. For the considered medium with randomly distributed inclusions, the multiscale coarse space does not perform noticeably better then the linear coarse space.

7 Discussion

In this report, we extended the (linear) multiscale finite element method to the (3D) PDE system of linear elasticity. The linear boundary conditions along coarse elements and the PDE-harmonic extension to their interior guarantees the following properties of the MsFEM basis:

1. Given the local boundary conditions, the energy of a multiscale basis function is minimal within each coarse element;
2. The 3 rigid body translations are contained in the coarse space;
3. The 3 rigid body rotations are contained in the coarse space;
4. Assuming homogeneous material coefficients, the multiscale basis coincides with the piecewise linear vector-valued basis on the coarse triangulation;

We utilized the multiscale basis for the construction of a two-level Additive Schwarz preconditioner. When the discontinuities are isolated in the interior of coarse elements, our experiments show uniform condition number bounds w.r.t. both, coefficient variations in the Young's modulus and the mesh size. Along coarse element boundaries, the multiscale basis is not PDE-harmonic. When inclusions cross a coarse element boundary, the prescribed linear boundary conditions lead to an increase in the energy of the multiscale basis function. The magnitude of the energy grows with the Young's modulus of the inclusions which cross the element boundaries. The condition number is not uniformly bounded. For the scalar case, it is shown in [12] that the robustness of an overlapping two-level Domain Decomposition method w.r.t coefficient variations is strongly related to the energy of the coarse basis functions. There, they introduce a *coarse space robustness indicator*, a measure which is proportional to the weighted H^1-seminorm of the basis functions. Our experimental results justify expectations to obtain similar condition number bounds for the PDE system of linear elasticity then existing ones for scalar elliptic PDEs. This correspondence will be investigated in more detail in a future work.

Using the MsFEM coarse space in an upscaling framework, we also presented experimental results in which we used the multiscale coarse space to approximate the fine-scale solution. When the inclusions are randomly distributed, the multiscale coarse space suffers from the inclusions which touch the coarse element boundaries and performs very similar to the linear coarse space. For the isolated inclusions, almost uniform approximation properties, independent of the contrast in the Young's modulus, were achieved.

However, along the boundaries of the coarse elements, the small scale heterogeneities cannot be captured accurately by the presented MsFEM coarse space with linear

boundary conditions. In case that material jumps occur through element boundaries, the coarse space needs to be adapted. A possible extension can be given using oscillatory boundary conditions, similar to the ones in scalar case (c.f. [14, 12]), or energy minimizing methods (c.f. [36, 31]). Attention has to be paid and modifications might be required such that translations as well as rotations remain in the coarse space. Another interesting approach is motivated and discussed in detail in [8], with application to scalar elliptic PDEs. There, local generalized eigenvalue problems are solved and a multiscale coarse space is extended by the remaining eigenfunctions corresponding to eigenvalues which lie under a predefined threshold. More recently, this approach is extended in [35] from a two-level to a multilevel method with an extension to general s.p.d. operators. A theoretical verification of the robustness of the method when applied to linear elasticity is also presented. Since the multiscale coarse space contains the rigid body modes, the paper at hand promises a reasonably low dimension of the coarse space presented in [35] for heterogeneous problems in (2D) linear elasticity.

Acknowledgements: The authors would like to thank Prof. Yalchin Efendiev for many fruitful discussions and his valuable comments on the subject of this report. Also, one of the authors acknowledges the participation at the "RICAM Special Semester on Multiscale Simulation & Analysis in Energy and the Environment (2011)" in Linz, Austria.

References

[1] A.H. Baker, T. Kolev, U.M. Yang, *Improving algebraic multigrid interpolation operators for linear elasticity problems*, Numer. Linear Algebra Appl., 17, (2010), 495–517.

[2] D. Braess, *Finite Elemente,* 3rd ed., Springer (2002).

[3] F. Brezzi, M. Fortin, *Mixed and hybrid finite element methods*, Springer (1991).

[4] T. Clees, *AMG Strategies for PDE Systems with Applications in Industrial Semiconductor Simulation*, PhD Dissertation, University of Cologne, Faculty of Mathematics (2005).

[5] Ph. Clément, *Approximation by finite element functions using local regularization*, RAIRO Anal. Numer., R-2, (1975), 77–84.

[6] N. Spillane, V. Dolean, P. Hauret, F. Nataf, C. Pechstein, R. Scheichl, *Abstract robust coarse spaces for systems of PDEs via generalized eigenproblems in the overlaps*, Technical Report 2011-07, University of Linz, Institute of Computational Mathematics (2011).

[7] L.J. Durlofsky, Y. Efendiev, V. Ginting, *An adaptive local-global multiscale finite volume element method for two-phase flow simulations*, Advances in Water Resources, 30, (2007), 576–588.

[8] Y. Efendiev, J. Galvis, R. Lazarov, J. Willems, *Robust domain decomposition preconditioners for abstract symmetric positive definite bilinear forms*, http://adsabs.harvard.edu/abs/2011arXiv1105.1131E (2011).

[9] Y. Efendiev, T.Y. Hou, *Multiscale finite element methods, theory and applications,* Surveys and Tutorials in the Applied Mathematical Sciences, 4th ed. (2009), 234 p.

[10] A. Ern, J.-L. Guermond, *Theory and practice of finite elements*, Applied Mathematical Sciences, 159, (2004), 524 p.

[11] R.S. Falk, *Non-conforming Finite element methods for the equations of linear elasticity*, Mathematics of Computations, 57, (1991), 529–550.

[12] I.G. Graham, P.O. Lechner, R. Scheichl, *Domain decomposition for multiscale PDEs*, Numer. Math., 106, (2007), 589–626.

[13] I.G. Graham, P.O. Lechner, R. Scheichl, *Robust domain decomposition algorithms for multiscale PDEs*, Numer. Methods Partial Differ. Equ., 23, (2007), 859–878.

[14] T.Y. Hou, X.H. Wu, *A multiscale finite element method for elliptic problems in composite materials and porous media,* J. Comput. Phys., 134, (1997), 169-189.

[15] T.Y. Hou, X.H. Wu, *A multiscale finite element method for PDEs with oscillatory coefficients,* Notes on Numerical Fluid Mechanics, 70, (1999), 58-69.

[16] T.Y. Hou, X.H. Wu, Z.-Cai, *Convergence of a multiscale finite element method for elliptic problems with rapidly oscillating coefficients,* Math. Comput., 68, (1999), 913-943.

[17] T.J.R. Hughes, *The finite element method: Linear static and dynamic finite element analysis*, Prentice-Hall, Inc. (1987).

[18] O. Iliev, R. Lazarov, and J. Willems, *Variational multiscale finite element method for flows in highly porous media*, Multiscale Model. Simul., 9, (2011), 1350-1372

[19] A. Janka, *Algebraic domain decomposition solver for linear elasticity*, Applications of Mathematics, 44, (1999), 435-458.

[20] E. Karer, *Subspace correction methods for linear elasticity*, PhD Dissertation, University of Linz (2011).

[21] E. Karer, J.K. Kraus, *Algebraic multigrid for finite element elasticity equations: Determination of nodal dependence via edge matrices and two-level convergence*, Int. J. Numer. Meth. Engng., 83, (2010), 642–670.

[22] T. Kolev, S. Margenov, *AMLI Preconditioning of pure displacement nonconforming elasticity FEM systems*, Numerical Analysis and its Applications, 1988, (2001), 339–367.

[23] J.K. Kraus, J. Schicho, *Algebraic multigrid based on computational molecules, I: Scalar elliptic problems*, Computing., 77, (2006), 57–75.

[24] J.K. Kraus, *Algebraic multigrid based on computational molecules, II: Linear elasticity problems*, SIAM J.Sci Comput., 30, (2008), 505–524.

[25] R. Millward, *A new adaptive multiscale finite element method with applications to high contrast interface problems*, PhD Dissertation, University of Bath (2011).

[26] Y. Saad, *Iterative methods for sparse linear systems,* 2nd ed., SIAM (2003).

[27] M. Sarkis, *Partition of unity coarse spaces: Enhanced versions, discontinuous coefficients and applications to elasticity,* Proceedings of 14th International Conference Domain Decomposition Methods, DDM (2003).

[28] V. Schulz, H. Andrä, K. Schmidt, *Robuste Netzgenerierung zur Mikro-FE-Analyse mikrostrukturierter Materialien*, NAFEMS Magazin 2 (2007), 28–30.

[29] B.F. Smith *Domain decomposition algorithms for the partial differential equations of linear elasticity*, PhD Dissertation, Courant Institute of Mathematical Sciences, New York University (1990).

[30] A. Toselli, O. Widlund, *Domain Decomposition methods, algorithms an theory*, Springer Verlag, Berlin-Heidelberg-New-York (2005).

[31] J. Van lent, R. Scheichl, I.G. Graham, *Energy-minimizing coarse spaces for two-level Schwarz methods for multiscale PDEs*, Numer. Linear Algebra Appl., 16, (2009), 775–799.

[32] P. Vanek, M. Brezina, R. Tezaur, *Fast multigrid solver*, Appl. Math., 40, (1995), 1–20.

[33] P. Vanek, *Acceleration of convergence of a two-level algorithm by smoothing transfer operator*, Appl. of Math., 37, (1992), 265–274.

[34] P. Vanek, M. Brezina, R. Tezaur, *Two-grid method for linear elasticity on unstructured meshes*, SIAM J. Sci Comput., 21 (1999), 900–923.

[35] J. Willems, *Robust multilevel methods for general symmetric positive definite operators*, Techinical Report 2012-06, RICAM Institute for Computational and Applied Mathematics (2012).

[36] J. Xu, L.T. Zikatanov, *On an energy minimizing basis in algebraic multigrid methods*, Comput. Vis. Sci., 7, (2004), 121–127.

[37] Y. Zhu, A. Brandt, *An efficient multigrid method for the simulation of high resolution elastic solids*, ACM Trans. Graph., 29, (2010), 1–18.

Published reports of the Fraunhofer ITWM

The PDF-files of the following reports are available under:
www.itwm.fraunhofer.de/de/zentral__berichte/berichte

1. D. Hietel, K. Steiner, J. Struckmeier
A Finite - Volume Particle Method for Compressible Flows
(19 pages, 1998)

2. M. Feldmann, S. Seibold
Damage Diagnosis of Rotors: Application of Hilbert Transform and Multi-Hypothesis Testing
Keywords: Hilbert transform, damage diagnosis, Kalman filtering, non-linear dynamics
(23 pages, 1998)

3. Y. Ben-Haim, S. Seibold
Robust Reliability of Diagnostic Multi-Hypothesis Algorithms: Application to Rotating Machinery
Keywords: Robust reliability, convex models, Kalman filtering, multi-hypothesis diagnosis, rotating machinery, crack diagnosis
(24 pages, 1998)

4. F.-Th. Lentes, N. Siedow
Three-dimensional Radiative Heat Transfer in Glass Cooling Processes
(23 pages, 1998)

5. A. Klar, R. Wegener
A hierarchy of models for multilane vehicular traffic
Part I: Modeling
(23 pages, 1998)

Part II: Numerical and stochastic investigations
(17 pages, 1998)

6. A. Klar, N. Siedow
Boundary Layers and Domain Decomposition for Radiative Heat Transfer and Diffusion Equations: Applications to Glass Manufacturing Processes
(24 pages, 1998)

7. I. Choquet
Heterogeneous catalysis modelling and numerical simulation in rarified gas flows Part I: Coverage locally at equilibrium
(24 pages, 1998)

8. J. Ohser, B. Steinbach, C. Lang
Efficient Texture Analysis of Binary Images
(17 pages, 1998)

9. J. Orlik
Homogenization for viscoelasticity of the integral type with aging and shrinkage
(20 pages, 1998)

10. J. Mohring
Helmholtz Resonators with Large Aperture
(21 pages, 1998)

11. H. W. Hamacher, A. Schöbel
On Center Cycles in Grid Graphs
(15 pages, 1998)

12. H. W. Hamacher, K.-H. Küfer
Inverse radiation therapy planning - a multiple objective optimisation approach
(14 pages, 1999)

13. C. Lang, J. Ohser, R. Hilfer
On the Analysis of Spatial Binary Images
(20 pages, 1999)

14. M. Junk
On the Construction of Discrete Equilibrium Distributions for Kinetic Schemes
(24 pages, 1999)

15. M. Junk, S. V. Raghurame Rao
A new discrete velocity method for Navier-Stokes equations
(20 pages, 1999)

16. H. Neunzert
Mathematics as a Key to Key Technologies
(39 pages, 1999)

17. J. Ohser, K. Sandau
Considerations about the Estimation of the Size Distribution in Wicksell's Corpuscle Problem
(18 pages, 1999)

18. E. Carrizosa, H. W. Hamacher, R. Klein, S. Nickel
Solving nonconvex planar location problems by finite dominating sets
Keywords: Continuous Location, Polyhedral Gauges, Finite Dominating Sets, Approximation, Sandwich Algorithm, Greedy Algorithm
(19 pages, 2000)

19. A. Becker
A Review on Image Distortion Measures
Keywords: Distortion measure, human visual system
(26 pages, 2000)

20. H. W. Hamacher, M. Labbé, S. Nickel, T. Sonneborn
Polyhedral Properties of the Uncapacitated Multiple Allocation Hub Location Problem
Keywords: integer programming, hub location, facility location, valid inequalities, facets, branch and cut
(21 pages, 2000)

21. H. W. Hamacher, A. Schöbel
Design of Zone Tariff Systems in Public Transportation
(30 pages, 2001)

22. D. Hietel, M. Junk, R. Keck, D. Teleaga
The Finite-Volume-Particle Method for Conservation Laws
(16 pages, 2001)

23. T. Bender, H. Hennes, J. Kalcsics, M. T. Melo, S. Nickel
Location Software and Interface with GIS and Supply Chain Management
Keywords: facility location, software development, geographical information systems, supply chain management
(48 pages, 2001)

24. H. W. Hamacher, S. A. Tjandra
Mathematical Modelling of Evacuation Problems: A State of Art
(44 pages, 2001)

25. J. Kuhnert, S. Tiwari
Grid free method for solving the Poisson equation
Keywords: Poisson equation, Least squares method, Grid free method
(19 pages, 2001)

26. T. Götz, H. Rave, D. Reinel-Bitzer, K. Steiner, H. Tiemeier
Simulation of the fiber spinning process
Keywords: Melt spinning, fiber model, Lattice Boltzmann, CFD
(19 pages, 2001)

27. A. Zemitis
On interaction of a liquid film with an obstacle
Keywords: impinging jets, liquid film, models, numerical solution, shape
(22 pages, 2001)

28. I. Ginzburg, K. Steiner
Free surface lattice-Boltzmann method to model the filling of expanding cavities by Bingham Fluids
Keywords: Generalized LBE, free-surface phenomena, interface boundary conditions, filling processes, Bingham viscoplastic model, regularized models
(22 pages, 2001)

29. H. Neunzert
»Denn nichts ist für den Menschen als Menschen etwas wert, was er nicht mit Leidenschaft tun kann«
Vortrag anlässlich der Verleihung des Akademiepreises des Landes Rheinland-Pfalz am 21.11.2001
Keywords: Lehre, Forschung, angewandte Mathematik, Mehrskalenanalyse, Strömungsmechanik
(18 pages, 2001)

30. J. Kuhnert, S. Tiwari
Finite pointset method based on the projection method for simulations of the incompressible Navier-Stokes equations
Keywords: Incompressible Navier-Stokes equations, Meshfree method, Projection method, Particle scheme, Least squares approximation
AMS subject classification: 76D05, 76M28
(25 pages, 2001)

31. R. Korn, M. Krekel
Optimal Portfolios with Fixed Consumption or Income Streams
Keywords: Portfolio optimisation, stochastic control, HJB equation, discretisation of control problems
(23 pages, 2002)

32. M. Krekel
Optimal portfolios with a loan dependent credit spread
Keywords: Portfolio optimisation, stochastic control, HJB equation, credit spread, log utility, power utility, non-linear wealth dynamics
(25 pages, 2002)

33. J. Ohser, W. Nagel, K. Schladitz
The Euler number of discretized sets – on the choice of adjacency in homogeneous lattices
Keywords: image analysis, Euler number, neighborhod relationships, cuboidal lattice
(32 pages, 2002)

34. I. Ginzburg, K. Steiner
Lattice Boltzmann Model for Free-Surface flow and Its Application to Filling Process in Casting
Keywords: Lattice Boltzmann models; free-surface phenomena; interface boundary conditions; filling processes; injection molding; volume of fluid method; interface boundary conditions; advection-schemes; upwind-schemes
(54 pages, 2002)

35. M. Günther, A. Klar, T. Materne, R. Wegener
Multivalued fundamental diagrams and stop and go waves for continuum traffic equations
Keywords: traffic flow, macroscopic equations, kinetic derivation, multivalued fundamental diagram, stop and go waves, phase transitions
(25 pages, 2002)

36. S. Feldmann, P. Lang, D. Prätzel-Wolters
Parameter influence on the zeros of network determinants
Keywords: Networks, Equicofactor matrix polynomials, Realization theory, Matrix perturbation theory
(30 pages, 2002)

37. K. Koch, J. Ohser, K. Schladitz
Spectral theory for random closed sets and estimating the covariance via frequency space
Keywords: Random set, Bartlett spectrum, fast Fourier transform, power spectrum
(28 pages, 2002)

38. D. d'Humières, I. Ginzburg
Multi-reflection boundary conditions for lattice Boltzmann models
Keywords: lattice Boltzmann equation, boudary condistions, bounce-back rule, Navier-Stokes equation
(72 pages, 2002)

39. R. Korn
Elementare Finanzmathematik
Keywords: Finanzmathematik, Aktien, Optionen, Portfolio-Optimierung, Börse, Lehrerweiterbildung, Mathematikunterricht
(98 pages, 2002)

40. J. Kallrath, M. C. Müller, S. Nickel
Batch Presorting Problems: Models and Complexity Results
Keywords: Complexity theory, Integer programming, Assigment, Logistics
(19 pages, 2002)

41. J. Linn
On the frame-invariant description of the phase space of the Folgar-Tucker equation
Key words: fiber orientation, Folgar-Tucker equation, injection molding
(5 pages, 2003)

42. T. Hanne, S. Nickel
A Multi-Objective Evolutionary Algorithm for Scheduling and Inspection Planning in Software Development Projects
Key words: multiple objective programming, project management and scheduling, software development, evolutionary algorithms, efficient set
(29 pages, 2003)

43. T. Bortfeld , K.-H. Küfer, M. Monz, A. Scherrer, C. Thieke, H. Trinkaus
Intensity-Modulated Radiotherapy - A Large Scale Multi-Criteria Programming Problem
Keywords: multiple criteria optimization, representative systems of Pareto solutions, adaptive triangulation, clustering and disaggregation techniques, visualization of Pareto solutions, medical physics, external beam radiotherapy planning, intensity modulated radiotherapy
(31 pages, 2003)

44. T. Halfmann, T. Wichmann
Overview of Symbolic Methods in Industrial Analog Circuit Design
Keywords: CAD, automated analog circuit design, symbolic analysis, computer algebra, behavioral modeling, system simulation, circuit sizing, macro modeling, differential-algebraic equations, index
(17 pages, 2003)

45. S. E. Mikhailov, J. Orlik
Asymptotic Homogenisation in Strength and Fatigue Durability Analysis of Composites
Keywords: multiscale structures, asymptotic homogenization, strength, fatigue, singularity, non-local conditions
(14 pages, 2003)

46. P. Domínguez-Marín, P. Hansen, N. Mladenovic , S. Nickel
Heuristic Procedures for Solving the Discrete Ordered Median Problem
Keywords: genetic algorithms, variable neighborhood search, discrete facility location
(31 pages, 2003)

47. N. Boland, P. Domínguez-Marín, S. Nickel, J. Puerto
Exact Procedures for Solving the Discrete Ordered Median Problem
Keywords: discrete location, Integer programming
(41 pages, 2003)

48. S. Feldmann, P. Lang
Padé-like reduction of stable discrete linear systems preserving their stability
Keywords: Discrete linear systems, model reduction, stability, Hankel matrix, Stein equation
(16 pages, 2003)

49. J. Kallrath, S. Nickel
A Polynomial Case of the Batch Presorting Problem
Keywords: batch presorting problem, online optimization, competetive analysis, polynomial algorithms, logistics
(17 pages, 2003)

50. T. Hanne, H. L. Trinkaus
knowCube for MCDM – Visual and Interactive Support for Multicriteria Decision Making
Key words: Multicriteria decision making, knowledge management, decision support systems, visual interfaces, interactive navigation, real-life applications.
(26 pages, 2003)

51. O. Iliev, V. Laptev
On Numerical Simulation of Flow Through Oil Filters
Keywords: oil filters, coupled flow in plain and porous media, Navier-Stokes, Brinkman, numerical simulation
(8 pages, 2003)

52. W. Dörfler, O. Iliev, D. Stoyanov, D. Vassileva
On a Multigrid Adaptive Refinement Solver for Saturated Non-Newtonian Flow in Porous Media
Keywords: Nonlinear multigrid, adaptive refinement, non-Newtonian flow in porous media
(17 pages, 2003)

53. S. Kruse
On the Pricing of Forward Starting Options under Stochastic Volatility
Keywords: Option pricing, forward starting options, Heston model, stochastic volatility, cliquet options
(11 pages, 2003)

54. O. Iliev, D. Stoyanov
Multigrid – adaptive local refinement solver for incompressible flows
Keywords: Navier-Stokes equations, incompressible flow, projection-type splitting, SIMPLE, multigrid methods, adaptive local refinement, lid-driven flow in a cavity
(37 pages, 2003)

55. V. Starikovicius
The multiphase flow and heat transfer in porous media
Keywords: Two-phase flow in porous media, various formulations, global pressure, multiphase mixture model, numerical simulation
(30 pages, 2003)

56. P. Lang, A. Sarishvili, A. Wirsen
Blocked neural networks for knowledge extraction in the software development process
Keywords: Blocked Neural Networks, Nonlinear Regression, Knowledge Extraction, Code Inspection
(21 pages, 2003)

57. H. Knaf, P. Lang, S. Zeiser
Diagnosis aiding in Regulation Thermography using Fuzzy Logic
Keywords: fuzzy logic,knowledge representation, expert system
(22 pages, 2003)

58. M. T. Melo, S. Nickel, F. Saldanha da Gama
Largescale models for dynamic multicommodity capacitated facility location
Keywords: supply chain management, strategic planning, dynamic location, modeling
(40 pages, 2003)

59. J. Orlik
Homogenization for contact problems with periodically rough surfaces
Keywords: asymptotic homogenization, contact problems
(28 pages, 2004)

60. A. Scherrer, K.-H. Küfer, M. Monz, F. Alonso, T. Bortfeld
IMRT planning on adaptive volume structures – a significant advance of computational complexity
Keywords: Intensity-modulated radiation therapy (IMRT), inverse treatment planning, adaptive volume structures, hierarchical clustering, local refinement, adaptive clustering, convex programming, mesh generation, multi-grid methods
(24 pages, 2004)

61. D. Kehrwald
Parallel lattice Boltzmann simulation of complex flows
Keywords: Lattice Boltzmann methods, parallel computing, microstructure simulation, virtual material design, pseudo-plastic fluids, liquid composite moulding
(12 pages, 2004)

62. O. Iliev, J. Linn, M. Moog, D. Niedziela, V. Starikovicius
On the Performance of Certain Iterative Solvers for Coupled Systems Arising in Discretization of Non-Newtonian Flow Equations

Keywords: Performance of iterative solvers, Preconditioners, Non-Newtonian flow
(17 pages, 2004)

63. R. Ciegis, O. Iliev, S. Rief, K. Steiner
On Modelling and Simulation of Different Regimes for Liquid Polymer Moulding
Keywords: Liquid Polymer Moulding, Modelling, Simulation, Infiltration, Front Propagation, non-Newtonian flow in porous media
(43 pages, 2004)

64. T. Hanne, H. Neu
Simulating Human Resources in Software Development Processes
Keywords: Human resource modeling, software process, productivity, human factors, learning curve
(14 pages, 2004)

65. O. Iliev, A. Mikelic, P. Popov
Fluid structure interaction problems in deformable porous media: Toward permeability of deformable porous media
Keywords: fluid-structure interaction, deformable porous media, upscaling, linear elasticity, stokes, finite elements
(28 pages, 2004)

66. F. Gaspar, O. Iliev, F. Lisbona, A. Naumovich, P. Vabishchevich
On numerical solution of 1-D poroelasticity equations in a multilayered domain
Keywords: poroelasticity, multilayered material, finite volume discretization, MAC type grid
(41 pages, 2004)

67. J. Ohser, K. Schladitz, K. Koch, M. Nöthe
Diffraction by image processing and its application in materials science
Keywords: porous microstructure, image analysis, random set, fast Fourier transform, power spectrum, Bartlett spectrum
(13 pages, 2004)

68. H. Neunzert
Mathematics as a Technology: Challenges for the next 10 Years
Keywords: applied mathematics, technology, modelling, simulation, visualization, optimization, glass processing, spinning processes, fiber-fluid interaction, trubulence effects, topological optimization, multicriteria optimization, Uncertainty and Risk, financial mathematics, Malliavin calculus, Monte-Carlo methods, virtual material design, filtration, bio-informatics, system biology
(29 pages, 2004)

69. R. Ewing, O. Iliev, R. Lazarov, A. Naumovich
On convergence of certain finite difference discretizations for 1D poroelasticity interface problems
Keywords: poroelasticity, multilayered material, finite volume discretizations, MAC type grid, error estimates
(26 pages,2004)

70. W. Dörfler, O. Iliev, D. Stoyanov, D. Vassileva
On Efficient Simulation of Non-Newtonian Flow in Saturated Porous Media with a Multigrid Adaptive Refinement Solver
Keywords: Nonlinear multigrid, adaptive renement, non-Newtonian in porous media
(25 pages, 2004)

71. J. Kalcsics, S. Nickel, M. Schröder
Towards a Unified Territory Design Approach – Applications, Algorithms and GIS Integration
Keywords: territory desgin, political districting, sales territory alignment, optimization algorithms, Geographical Information Systems
(40 pages, 2005)

72. K. Schladitz, S. Peters, D. Reinel-Bitzer, A. Wiegmann, J. Ohser
Design of acoustic trim based on geometric modeling and flow simulation for non-woven
Keywords: random system of fibers, Poisson line process, flow resistivity, acoustic absorption, Lattice-Boltzmann method, non-woven
(21 pages, 2005)

73. V. Rutka, A. Wiegmann
Explicit Jump Immersed Interface Method for virtual material design of the effective elastic moduli of composite materials
Keywords: virtual material design, explicit jump immersed interface method, effective elastic moduli, composite materials
(22 pages, 2005)

74. T. Hanne
Eine Übersicht zum Scheduling von Baustellen
Keywords: Projektplanung, Scheduling, Bauplanung, Bauindustrie
(32 pages, 2005)

75. J. Linn
The Folgar-Tucker Model as a Differetial Algebraic System for Fiber Orientation Calculation
Keywords: fiber orientation, Folgar–Tucker model, invariants, algebraic constraints, phase space, trace stability
(15 pages, 2005)

76. M. Speckert, K. Dreßler, H. Mauch, A. Lion, G. J. Wierda
Simulation eines neuartigen Prüfsystems für Achserprobungen durch MKS-Modellierung einschließlich Regelung
Keywords: virtual test rig, suspension testing, multibody simulation, modeling hexapod test rig, optimization of test rig configuration
(20 pages, 2005)

77. K.-H. Küfer, M. Monz, A. Scherrer, P. Süss, F. Alonso, A. S. A. Sultan, Th. Bortfeld, D. Craft, Chr. Thieke
Multicriteria optimization in intensity modulated radiotherapy planning
Keywords: multicriteria optimization, extreme solutions, real-time decision making, adaptive approximation schemes, clustering methods, IMRT planning, reverse engineering
(51 pages, 2005)

78. S. Amstutz, H. Andrä
A new algorithm for topology optimization using a level-set method
Keywords: shape optimization, topology optimization, topological sensitivity, level-set
(22 pages, 2005)

79. N. Ettrich
Generation of surface elevation models for urban drainage simulation
Keywords: Flooding, simulation, urban elevation models, laser scanning
(22 pages, 2005)

80. H. Andrä, J. Linn, I. Matei, I. Shklyar, K. Steiner, E. Teichmann
OPTCAST – Entwicklung adäquater Strukturoptimierungsverfahren für Gießereien Technischer Bericht (KURZFASSUNG)
Keywords: Topologieoptimierung, Level-Set-Methode, Gießprozesssimulation, Gießtechnische Restriktionen, CAE-Kette zur Strukturoptimierung
(77 pages, 2005)

81. N. Marheineke, R. Wegener
Fiber Dynamics in Turbulent Flows Part I: General Modeling Framework
Keywords: fiber-fluid interaction; Cosserat rod; turbulence modeling; Kolmogorov's energy spectrum; double-velocity correlations; differentiable Gaussian fields
(20 pages, 2005)

Part II: Specific Taylor Drag
Keywords: flexible fibers; k-ε turbulence model; fiber-turbulence interaction scales; air drag; random Gaussian aerodynamic force; white noise; stochastic differential equations; ARMA process
(18 pages, 2005)

82. C. H. Lampert, O. Wirjadi
An Optimal Non-Orthogonal Separation of the Anisotropic Gaussian Convolution Filter
Keywords: Anisotropic Gaussian filter, linear filtering, orientation space, nD image processing, separable filters
(25 pages, 2005)

83. H. Andrä, D. Stoyanov
Error indicators in the parallel finite element solver for linear elasticity DDFEM
Keywords: linear elasticity, finite element method, hierarchical shape functions, domain decom-position, parallel implementation, a posteriori error estimates
(21 pages, 2006)

84. M. Schröder, I. Solchenbach
Optimization of Transfer Quality in Regional Public Transit
Keywords: public transit, transfer quality, quadratic assignment problem
(16 pages, 2006)

85. A. Naumovich, F. J. Gaspar
On a multigrid solver for the three-dimensional Biot poroelasticity system in multilayered domains
Keywords: poroelasticity, interface problem, multigrid, operator-dependent prolongation
(11 pages, 2006)

86. S. Panda, R. Wegener, N. Marheineke
Slender Body Theory for the Dynamics of Curved Viscous Fibers
Keywords: curved viscous fibers; fluid dynamics; Navier-Stokes equations; free boundary value problem; asymptotic expansions; slender body theory
(14 pages, 2006)

87. E. Ivanov, H. Andrä, A. Kudryavtsev
Domain Decomposition Approach for Automatic Parallel Generation of Tetrahedral Grids
Key words: Grid Generation, Unstructured Grid, Delaunay Triangulation, Parallel Programming, Domain Decomposition, Load Balancing
(18 pages, 2006)

88. S. Tiwari, S. Antonov, D. Hietel, J. Kuhnert, R. Wegener
A Meshfree Method for Simulations of Interactions between Fluids and Flexible Structures
Key words: Meshfree Method, FPM, Fluid Structure Interaction, Sheet of Paper, Dynamical Coupling
(16 pages, 2006)

89. R. Ciegis , O. Iliev, V. Starikovicius, K. Steiner
Numerical Algorithms for Solving Problems of Multiphase Flows in Porous Media
Keywords: nonlinear algorithms, finite-volume method, software tools, porous media, flows
(16 pages, 2006)

90. D. Niedziela, O. Iliev, A. Latz
On 3D Numerical Simulations of Viscoelastic Fluids
Keywords: non-Newtonian fluids, anisotropic viscosity, integral constitutive equation
(18 pages, 2006)

91. A. Winterfeld
Application of general semi-infinite Programming to Lapidary Cutting Problems
Keywords: large scale optimization, nonlinear programming, general semi-infinite optimization, design centering, clustering
(26 pages, 2006)

92. J. Orlik, A. Ostrovska
Space-Time Finite Element Approximation and Numerical Solution of Hereditary Linear Viscoelasticity Problems
Keywords: hereditary viscoelasticity; kern approximation by interpolation; space-time finite element approximation, stability and a priori estimate
(24 pages, 2006)

93. V. Rutka, A. Wiegmann, H. Andrä
EJIIM for Calculation of effective Elastic Moduli in 3D Linear Elasticity
Keywords: Elliptic PDE, linear elasticity, irregular domain, finite differences, fast solvers, effective elastic moduli
(24 pages, 2006)

94. A. Wiegmann, A. Zemitis
EJ-HEAT: A Fast Explicit Jump Harmonic Averaging Solver for the Effective Heat Conductivity of Composite Materials
Keywords: Stationary heat equation, effective thermal conductivity, explicit jump, discontinuous coefficients, virtual material design, microstructure simulation, EJ-HEAT
(21 pages, 2006)

95. A. Naumovich
On a finite volume discretization of the three-dimensional Biot poroelasticity system in multilayered domains
Keywords: Biot poroelasticity system, interface problems, finite volume discretization, finite difference method
(21 pages, 2006)

96. M. Krekel, J. Wenzel
A unified approach to Credit Default Swaption and Constant Maturity Credit Default Swap valuation
Keywords: LIBOR market model, credit risk, Credit Default Swaption, Constant Maturity Credit Default Swap-method
(43 pages, 2006)

97. A. Dreyer
Interval Methods for Analog Circiuts
Keywords: interval arithmetic, analog circuits, tolerance analysis, parametric linear systems, frequency response, symbolic analysis, CAD, computer algebra
(36 pages, 2006)

98. N. Weigel, S. Weihe, G. Bitsch, K. Dreßler
Usage of Simulation for Design and Optimization of Testing
Keywords: Vehicle test rigs, MBS, control, hydraulics, testing philosophy
(14 pages, 2006)

99. H. Lang, G. Bitsch, K. Dreßler, M. Speckert
Comparison of the solutions of the elastic and elastoplastic boundary value problems
Keywords: Elastic BVP, elastoplastic BVP, variational inequalities, rate-independency, hysteresis, linear kinematic hardening, stop- and play-operator
(21 pages, 2006)

100. M. Speckert, K. Dreßler, H. Mauch
MBS Simulation of a hexapod based suspension test rig
Keywords: Test rig, MBS simulation, suspension, hydraulics, controlling, design optimization
(12 pages, 2006)

101. S. Azizi Sultan, K.-H. Küfer
A dynamic algorithm for beam orientations in multicriteria IMRT planning
Keywords: radiotherapy planning, beam orientation optimization, dynamic approach, evolutionary algorithm, global optimization
(14 pages, 2006)

102. T. Götz, A. Klar, N. Marheineke, R. Wegener
A Stochastic Model for the Fiber Lay-down Process in the Nonwoven Production
Keywords: fiber dynamics, stochastic Hamiltonian system, stochastic averaging
(17 pages, 2006)

103. Ph. Süss, K.-H. Küfer
Balancing control and simplicity: a variable aggregation method in intensity modulated radiation therapy planning
Keywords: IMRT planning, variable aggregation, clustering methods
(22 pages, 2006)

104. A. Beaudry, G. Laporte, T. Melo, S. Nickel
Dynamic transportation of patients in hospitals
Keywords: in-house hospital transportation, dial-a-ride, dynamic mode, tabu search
(37 pages, 2006)

105. Th. Hanne
Applying multiobjective evolutionary algorithms in industrial projects
Keywords: multiobjective evolutionary algorithms, discrete optimization, continuous optimization, electronic circuit design, semi-infinite programming, scheduling
(18 pages, 2006)

106. J. Franke, S. Halim
Wild bootstrap tests for comparing signals and images
Keywords: wild bootstrap test, texture classification, textile quality control, defect detection, kernel estimate, nonparametric regression
(13 pages, 2007)

107. Z. Drezner, S. Nickel
Solving the ordered one-median problem in the plane
Keywords: planar location, global optimization, ordered median, big triangle small triangle method, bounds, numerical experiments
(21 pages, 2007)

108. Th. Götz, A. Klar, A. Unterreiter, R. Wegener
Numerical evidance for the non-existing of solutions of the equations desribing rotational fiber spinning
Keywords: rotational fiber spinning, viscous fibers, boundary value problem, existence of solutions
(11 pages, 2007)

109. Ph. Süss, K.-H. Küfer
Smooth intensity maps and the Bortfeld-Boyer sequencer
Keywords: probabilistic analysis, intensity modulated radiotherapy treatment (IMRT), IMRT plan application, step-and-shoot sequencing
(8 pages, 2007)

110. E. Ivanov, O. Gluchshenko, H. Andrä, A. Kudryavtsev
Parallel software tool for decomposing and meshing of 3d structures
Keywords: a-priori domain decomposition, unstructured grid, Delaunay mesh generation
(14 pages, 2007)

111. O. Iliev, R. Lazarov, J. Willems
Numerical study of two-grid preconditioners for 1d elliptic problems with highly oscillating discontinuous coefficients
Keywords: two-grid algorithm, oscillating coefficients, preconditioner
(20 pages, 2007)

112. L. Bonilla, T. Götz, A. Klar, N. Marheineke, R. Wegener
Hydrodynamic limit of the Fokker-Planck-equation describing fiber lay-down processes
Keywords: stochastic dierential equations, Fokker-Planck equation, asymptotic expansion, Ornstein-Uhlenbeck process
(17 pages, 2007)

113. S. Rief
Modeling and simulation of the pressing section of a paper machine
Keywords: paper machine, computational fluid dynamics, porous media
(41 pages, 2007)

114. R. Ciegis, O. Iliev, Z. Lakdawala
On parallel numerical algorithms for simulating industrial filtration problems
Keywords: Navier-Stokes-Brinkmann equations, finite volume discretization method, SIMPLE, parallel computing, data decomposition method
(24 pages, 2007)

115. N. Marheineke, R. Wegener
Dynamics of curved viscous fibers with surface tension
Keywords: Slender body theory, curved viscous bers with surface tension, free boundary value problem
(25 pages, 2007)

116. S. Feth, J. Franke, M. Speckert
Resampling-Methoden zur mse-Korrektur und Anwendungen in der Betriebsfestigkeit
Keywords: Weibull, Bootstrap, Maximum-Likelihood, Betriebsfestigkeit
(16 pages, 2007)

117. H. Knaf
Kernel Fisher discriminant functions – a concise and rigorous introduction
Keywords: wild bootstrap test, texture classification, textile quality control, defect detection, kernel estimate, nonparametric regression
(30 pages, 2007)

118. O. Iliev, I. Rybak
On numerical upscaling for flows in heterogeneous porous media

Keywords: numerical upscaling, heterogeneous porous media, single phase flow, Darcy's law, multiscale problem, effective permeability, multipoint flux approximation, anisotropy
(17 pages, 2007)

119. O. Iliev, I. Rybak
On approximation property of multipoint flux approximation method
Keywords: Multipoint flux approximation, finite volume method, elliptic equation, discontinuous tensor coefficients, anisotropy
(15 pages, 2007)

120. O. Iliev, I. Rybak, J. Willems
On upscaling heat conductivity for a class of industrial problems
Keywords: Multiscale problems, effective heat conductivity, numerical upscaling, domain decomposition
(21 pages, 2007)

121. R. Ewing, O. Iliev, R. Lazarov, I. Rybak
On two-level preconditioners for flow in porous media
Keywords: Multiscale problem, Darcy's law, single phase flow, anisotropic heterogeneous porous media, numerical upscaling, multigrid, domain decomposition, efficient preconditioner
(18 pages, 2007)

122. M. Brickenstein, A. Dreyer
POLYBORI: A Gröbner basis framework for Boolean polynomials
Keywords: Gröbner basis, formal verification, Boolean polynomials, algebraic cryptoanalysis, satisfiability
(23 pages, 2007)

123. O. Wirjadi
Survey of 3d image segmentation methods
Keywords: image processing, 3d, image segmentation, binarization
(20 pages, 2007)

124. S. Zeytun, A. Gupta
A Comparative Study of the Vasicek and the CIR Model of the Short Rate
Keywords: interest rates, Vasicek model, CIR-model, calibration, parameter estimation
(17 pages, 2007)

125. G. Hanselmann, A. Sarishvili
Heterogeneous redundancy in software quality prediction using a hybrid Bayesian approach
Keywords: reliability prediction, fault prediction, non-homogeneous poisson process, Bayesian model averaging
(17 pages, 2007)

126. V. Maag, M. Berger, A. Winterfeld, K.-H. Küfer
A novel non-linear approach to minimal area rectangular packing
Keywords: rectangular packing, non-overlapping constraints, non-linear optimization, regularization, relaxation
(18 pages, 2007)

127. M. Monz, K.-H. Küfer, T. Bortfeld, C. Thieke
Pareto navigation – systematic multi-criteria-based IMRT treatment plan determination
Keywords: convex, interactive multi-objective optimization, intensity modulated radiotherapy planning
(15 pages, 2007)

128. M. Krause, A. Scherrer
On the role of modeling parameters in IMRT plan optimization
Keywords: intensity-modulated radiotherapy (IMRT), inverse IMRT planning, convex optimization, sensitivity analysis, elasticity, modeling parameters, equivalent uniform dose (EUD)
(18 pages, 2007)

129. A. Wiegmann
Computation of the permeability of porous materials from their microstructure by FFF-Stokes
Keywords: permeability, numerical homogenization, fast Stokes solver
(24 pages, 2007)

130. T. Melo, S. Nickel, F. Saldanha da Gama
Facility Location and Supply Chain Management – A comprehensive review
Keywords: facility location, supply chain management, network design
(54 pages, 2007)

131. T. Hanne, T. Melo, S. Nickel
Bringing robustness to patient flow management through optimized patient transports in hospitals
Keywords: Dial-a-Ride problem, online problem, case study, tabu search, hospital logistics
(23 pages, 2007)

132. R. Ewing, O. Iliev, R. Lazarov, I. Rybak, J. Willems
An efficient approach for upscaling properties of composite materials with high contrast of coefficients
Keywords: effective heat conductivity, permeability of fractured porous media, numerical upscaling, fibrous insulation materials, metal foams
(16 pages, 2008)

133. S. Gelareh, S. Nickel
New approaches to hub location problems in public transport planning
Keywords: integer programming, hub location, transportation, decomposition, heuristic
(25 pages, 2008)

134. G. Thömmes, J. Becker, M. Junk, A. K. Vaikuntam, D. Kehrwald, A. Klar, K. Steiner, A. Wiegmann
A Lattice Boltzmann Method for immiscible multiphase flow simulations using the Level Set Method
Keywords: Lattice Boltzmann method, Level Set method, free surface, multiphase flow
(28 pages, 2008)

135. J. Orlik
Homogenization in elasto-plasticity
Keywords: multiscale structures, asymptotic homogenization, nonlinear energy
(40 pages, 2008)

136. J. Almquist, H. Schmidt, P. Lang, J. Deitmer, M. Jirstrand, D. Prätzel-Wolters, H. Becker
Determination of interaction between MCT1 and CAII via a mathematical and physiological approach
Keywords: mathematical modeling; model reduction; electrophysiology; pH-sensitive microelectrodes; proton antenna
(20 pages, 2008)

137. E. Savenkov, H. Andrä, O. Iliev
An analysis of one regularization approach for solution of pure Neumann problem
Keywords: pure Neumann problem, elasticity, regularization, finite element method, condition number
(27 pages, 2008)

138. O. Berman, J. Kalcsics, D. Krass, S. Nickel
The ordered gradual covering location problem on a network
Keywords: gradual covering, ordered median function, network location
(32 pages, 2008)

139. S. Gelareh, S. Nickel
Multi-period public transport design: A novel model and solution approaches
Keywords: Integer programming, hub location, public transport, multi-period planning, heuristics
(31 pages, 2008)

140. T. Melo, S. Nickel, F. Saldanha-da-Gama
Network design decisions in supply chain planning
Keywords: supply chain design, integer programming models, location models, heuristics
(20 pages, 2008)

141. C. Lautensack, A. Särkkä, J. Freitag, K. Schladitz
Anisotropy analysis of pressed point processes
Keywords: estimation of compression, isotropy test, nearest neighbour distance, orientation analysis, polar ice, Ripley's K function
(35 pages, 2008)

142. O. Iliev, R. Lazarov, J. Willems
A Graph-Laplacian approach for calculating the effective thermal conductivity of complicated fiber geometries
Keywords: graph laplacian, effective heat conductivity, numerical upscaling, fibrous materials
(14 pages, 2008)

143. J. Linn, T. Stephan, J. Carlsson, R. Bohlin
Fast simulation of quasistatic rod deformations for VR applications
Keywords: quasistatic deformations, geometrically exact rod models, variational formulation, energy minimization, finite differences, nonlinear conjugate gradients
(7 pages, 2008)

144. J. Linn, T. Stephan
Simulation of quasistatic deformations using discrete rod models
Keywords: quasistatic deformations, geometrically exact rod models, variational formulation, energy minimization, finite differences, nonlinear conjugate gradients
(9 pages, 2008)

145. J. Marburger, N. Marheineke, R. Pinnau
Adjoint based optimal control using mesh-less discretizations
Keywords: Mesh-less methods, particle methods, Eulerian-Lagrangian formulation, optimization strategies, adjoint method, hyperbolic equations
(14 pages, 2008

146. S. Desmettre, J. Gould, A. Szimayer
Own-company stockholding and work effort preferences of an unconstrained executive
Keywords: optimal portfolio choice, executive compensation
(33 pages, 2008)

147. M. Berger, M. Schröder, K.-H. Küfer
A constraint programming approach for the two-dimensional rectangular packing problem with orthogonal orientations
Keywords: rectangular packing, orthogonal orientations non-overlapping constraints, constraint propagation
(13 pages, 2008)

148. K. Schladitz, C. Redenbach, T. Sych, M. Godehardt
Microstructural characterisation of open foams using 3d images
Keywords: virtual material design, image analysis, open foams
(30 pages, 2008)

149. E. Fernández, J. Kalcsics, S. Nickel, R. Ríos-Mercado
A novel territory design model arising in the implementation of the WEEE-Directive
Keywords: heuristics, optimization, logistics, recycling
(28 pages, 2008)

150. H. Lang, J. Linn
Lagrangian field theory in space-time for geometrically exact Cosserat rods
Keywords: Cosserat rods, geometrically exact rods, small strain, large deformation, deformable bodies, Lagrangian field theory, variational calculus
(19 pages, 2009)

151. K. Dreßler, M. Speckert, R. Müller, Ch. Weber
Customer loads correlation in truck engineering
Keywords: Customer distribution, safety critical components, quantile estimation, Monte-Carlo methods
(11 pages, 2009)

152. H. Lang, K. Dreßler
An improved multiaxial stress-strain correction model for elastic FE postprocessing
Keywords: Jiang's model of elastoplasticity, stress-strain correction, parameter identification, automatic differentiation, least-squares optimization, Coleman-Li algorithm
(6 pages, 2009)

153. J. Kalcsics, S. Nickel, M. Schröder
A generic geometric approach to territory design and districting
Keywords: Territory design, districting, combinatorial optimization, heuristics, computational geometry
(32 pages, 2009)

154. Th. Fütterer, A. Klar, R. Wegener
An energy conserving numerical scheme for the dynamics of hyperelastic rods
Keywords: Cosserat rod, hyperealstic, energy conservation, finite differences
(16 pages, 2009)

155. A. Wiegmann, L. Cheng, E. Glatt, O. Iliev, S. Rief
Design of pleated filters by computer simulations
Keywords: Solid-gas separation, solid-liquid separation, pleated filter, design, simulation
(21 pages, 2009)

156. A. Klar, N. Marheineke, R. Wegener
Hierarchy of mathematical models for production processes of technical textiles
Keywords: Fiber-fluid interaction, slender-body theory, turbulence modeling, model reduction, stochastic differential equations, Fokker-Planck equation, asymptotic expansions, parameter identification
(21 pages, 2009)

157. E. Glatt, S. Rief, A. Wiegmann, M. Knefel, E. Wegenke
Structure and pressure drop of real and virtual metal wire meshes
Keywords: metal wire mesh, structure simulation, model calibration, CFD simulation, pressure loss
(7 pages, 2009)

158. S. Kruse, M. Müller
Pricing American call options under the assumption of stochastic dividends – An application of the Korn-Rogers model
Keywords: option pricing, American options, dividends, dividend discount model, Black-Scholes model
(22 pages, 2009)

159. H. Lang, J. Linn, M. Arnold
Multibody dynamics simulation of geometrically exact Cosserat rods
Keywords: flexible multibody dynamics, large deformations, finite rotations, constrained mechanical systems, structural dynamics
(20 pages, 2009)

160. P. Jung, S. Leyendecker, J. Linn, M. Ortiz
Discrete Lagrangian mechanics and geometrically exact Cosserat rods
Keywords: special Cosserat rods, Lagrangian mechanics, Noether's theorem, discrete mechanics, frame-indifference, holonomic constraints
(14 pages, 2009)

161. M. Burger, K. Dreßler, A. Marquardt, M. Speckert
Calculating invariant loads for system simulation in vehicle engineering
Keywords: iterative learning control, optimal control theory, differential algebraic equations (DAEs)
(18 pages, 2009)

162. M. Speckert, N. Ruf, K. Dreßler
Undesired drift of multibody models excited by measured accelerations or forces
Keywords: multibody simulation, full vehicle model, force-based simulation, drift due to noise
(19 pages, 2009)

163. A. Streit, K. Dreßler, M. Speckert, J. Lichter, T. Zenner, P. Bach
Anwendung statistischer Methoden zur Erstellung von Nutzungsprofilen für die Auslegung von Mobilbaggern
Keywords: Nutzungsvielfalt, Kundenbeanspruchung, Bemessungsgrundlagen
(13 pages, 2009)

164. I. Correia, S. Nickel, F. Saldanha-da-Gama
The capacitated single-allocation hub location problem revisited: A note on a classical formulation
Keywords: Capacitated Hub Location, MIP formulations
(10 pages, 2009)

165. F. Yaneva, T. Grebe, A. Scherrer
An alternative view on global radiotherapy optimization problems
Keywords: radiotherapy planning, path-connected sublevelsets, modified gradient projection method, improving and feasible directions
(14 pages, 2009)

166. J. I. Serna, M. Monz, K.-H. Küfer, C. Thieke
Trade-off bounds and their effect in multi-criteria IMRT planning
Keywords: trade-off bounds, multi-criteria optimization, IMRT, Pareto surface
(15 pages, 2009)

167. W. Arne, N. Marheineke, A. Meister, R. Wegener
Numerical analysis of Cosserat rod and string models for viscous jets in rotational spinning processes
Keywords: Rotational spinning process, curved viscous fibers, asymptotic Cosserat models, boundary value problem, existence of numerical solutions
(18 pages, 2009)

168. T. Melo, S. Nickel, F. Saldanha-da-Gama
An LP-rounding heuristic to solve a multi-period facility relocation problem
Keywords: supply chain design, heuristic, linear programming, rounding
(37 pages, 2009)

169. I. Correia, S. Nickel, F. Saldanha-da-Gama
Single-allocation hub location problems with capacity choices
Keywords: hub location, capacity decisions, MILP formulations
(27 pages, 2009)

170. S. Acar, K. Natcheva-Acar
A guide on the implementation of the Heath-Jarrow-Morton Two-Factor Gaussian Short Rate Model (HJM-G2++)
Keywords: short rate model, two factor Gaussian, G2++, option pricing, calibration
(30 pages, 2009)

171. A. Szimayer, G. Dimitroff, S. Lorenz
A parsimonious multi-asset Heston model: calibration and derivative pricing
Keywords: Heston model, multi-asset, option pricing, calibration, correlation
(28 pages, 2009)

172. N. Marheineke, R. Wegener
Modeling and validation of a stochastic drag for fibers in turbulent flows
Keywords: fiber-fluid interactions, long slender fibers, turbulence modelling, aerodynamic drag, dimensional analysis, data interpolation, stochastic partial differential algebraic equation, numerical simulations, experimental validations
(19 pages, 2009)

173. S. Nickel, M. Schröder, J. Steeg
Planning for home health care services
Keywords: home health care, route planning, metaheuristics, constraint programming
(23 pages, 2009)

174. G. Dimitroff, A. Szimayer, A. Wagner
Quanto option pricing in the parsimonious Heston model
Keywords: Heston model, multi asset, quanto options, option pricing
(14 pages, 2009) 174. G. Dimitroff, A. Szimayer, A. Wagner

175. S. Herkt, K. Dreßler, R. Pinnau
Model reduction of nonlinear problems in structural mechanics
Keywords: flexible bodies, FEM, nonlinear model reduction, POD
(13 pages, 2009)

176. M. K. Ahmad, S. Didas, J. Iqbal
Using the Sharp Operator for edge detection and nonlinear diffusion
Keywords: maximal function, sharp function,image processing, edge detection, nonlinear diffusion
(17 pages, 2009)

177. M. Speckert, N. Ruf, K. Dreßler, R. Müller, C. Weber, S. Weihe
Ein neuer Ansatz zur Ermittlung von Erprobungslasten für sicherheitsrelevante Bauteile
Keywords: sicherheitsrelevante Bauteile, Kundenbeanspruchung, Festigkeitsverteilung, Ausfallwahrscheinlichkeit, Konfidenz, statistische Unsicherheit, Sicherheitsfaktoren
(16 pages, 2009)

178. J. Jegorovs
Wave based method: new applicability areas
Keywords: Elliptic boundary value problems, inhomogeneous Helmholtz type differential equations in bounded domains, numerical methods, wave based method, uniform B-splines
(10 pages, 2009)

179. H. Lang, M. Arnold
Numerical aspects in the dynamic simulation of geometrically exact rods
Keywords: Kirchhoff and Cosserat rods, geometrically exact rods, deformable bodies, multibody dynamics,artial differential algebraic equations, method of lines, time integration
(21 pages, 2009)

180. H. Lang
Comparison of quaternionic and rotation-free null space formalisms for multibody dynamics
Keywords: Parametrisation of rotations, differential-algebraic equations, multibody dynamics, constrained mechanical systems, Lagrangian mechanics
(40 pages, 2010)

181. S. Nickel, F. Saldanha-da-Gama, H.-P. Ziegler
Stochastic programming approaches for risk aware supply chain network design problems
Keywords: Supply Chain Management, multi-stage stochastic programming, financial decisions, risk
(37 pages, 2010)

182. P. Ruckdeschel, N. Horbenko
Robustness properties of estimators in generalized Pareto Models
Keywords: global robustness, local robustness, finite sample breakdown point, generalized Pareto distribution
(58 pages, 2010)

183. P. Jung, S. Leyendecker, J. Linn, M. Ortiz
A discrete mechanics approach to Cosserat rod theory – Part 1: static equilibria
Keywords: Special Cosserat rods; Lagrangian mechanics; Noether's theorem; discrete mechanics; frame-indifference; holonomic constraints; variational formulation
(35 pages, 2010)

184. R. Eymard, G. Printsypar
A proof of convergence of a finite volume scheme for modified steady Richards' equation describing transport processes in the pressing section of a paper machine
Keywords: flow in porous media, steady Richards' equation, finite volume methods, convergence of approximate solution
(14 pages, 2010)

185. P. Ruckdeschel
Optimally Robust Kalman Filtering
Keywords: robustness, Kalman Filter, innovation outlier, additive outlier
(42 pages, 2010)

186. S. Repke, N. Marheineke, R. Pinnau
On adjoint-based optimization of a free surface Stokes flow
Keywords: film casting process, thin films, free surface Stokes flow, optimal control, Lagrange formalism
(13 pages, 2010)

187. O. Iliev, R. Lazarov, J. Willems
Variational multiscale Finite Element Method for flows in highly porous media
Keywords: numerical upscaling, flow in heterogeneous porous media, Brinkman equations, Darcy's law, subgrid approximation, discontinuous Galerkin mixed FEM
(21 pages, 2010)

188. S. Desmettre, A. Szimayer
Work effort, consumption, and portfolio selection: When the occupational choice matters
Keywords: portfolio choice, work effort, consumption, occupational choice
(34 pages, 2010)

189. O. Iliev, Z. Lakdawala, V. Starikovicius
On a numerical subgrid upscaling algorithm for Stokes-Brinkman equations
Keywords: Stokes-Brinkman equations, subgrid approach, multiscale problems, numerical upscaling
(27 pages, 2010)

190. A. Latz, J. Zausch, O. Iliev
Modeling of species and charge transport in Li-Ion Batteries based on non-equilibrium thermodynamics
Keywords: lithium-ion battery, battery modeling, electrochemical simulation, concentrated electrolyte, ion transport
(8 pages, 2010)

191. P. Popov, Y. Vutov, S. Margenov, O. Iliev
Finite volume discretization of equations describing nonlinear diffusion in Li-Ion batteries
Keywords: nonlinear diffusion, finite volume discretization, Newton method, Li-Ion batteries
(9 pages, 2010)

192. W. Arne, N. Marheineke, R. Wegener
Asymptotic transition from Cosserat rod to string models for curved viscous inertial jets
Keywords: rotational spinning processes; inertial and viscous-inertial fiber regimes; asymptotic limits; slender-body theory; boundary value problems
(23 pages, 2010)

193. L. Engelhardt, M. Burger, G. Bitsch
Real-time simulation of multibody-systems for on-board applications
Keywords: multibody system simulation, real-time simulation, on-board simulation, Rosenbrock methods
(10 pages, 2010)

194. M. Burger, M. Speckert, K. Dreßler
Optimal control methods for the calculation of invariant excitation signals for multibody systems
Keywords: optimal control, optimization, mbs simulation, invariant excitation
(9 pages, 2010)

195. A. Latz, J. Zausch
Thermodynamic consistent transport theory of Li-Ion batteries
Keywords: Li-Ion batteries, nonequilibrium thermodynamics, thermal transport, modeling
(18 pages, 2010)

196. S. Desmettre
Optimal investment for executive stockholders with exponential utility
Keywords: portfolio choice, executive stockholder, work effort, exponential utility
(24 pages, 2010)

197. W. Arne, N. Marheineke, J. Schnebele, R. Wegener
Fluid-fiber-interactions in rotational spinning process of glass wool production
Keywords: Rotational spinning process, viscous thermal jets, fluid-fiber-interactions, two-way coupling, slender-body theory, Cosserat rods, drag models, boundary value problem, continuation method
(20 pages, 2010)

198. A. Klar, J. Maringer, R. Wegener
A 3d model for fiber lay-down in nonwoven production processes
Keywords: fiber dynamics, Fokker-Planck equations, diffusion limits
(15 pages, 2010)

199. Ch. Erlwein, M. Müller
A regime-switching regression model for hedge funds
Keywords: switching regression model, Hedge funds, optimal parameter estimation, filtering
(26 pages, 2011)

200. M. Dalheimer
Power to the people – Das Stromnetz der Zukunft
Keywords: Smart Grid, Stromnetz, Erneuerbare Energien, Demand-Side Management
(27 pages, 2011)

201. D. Stahl, J. Hauth
PF-MPC: Particle Filter-Model Predictive Control
Keywords: Model Predictive Control, Particle Filter, CSTR, Inverted Pendulum, Nonlinear Systems, Sequential Monte Carlo
(40 pages, 2011)

202. G. Dimitroff, J. de Kock
Calibrating and completing the volatility cube in the SABR Model
Keywords: stochastic volatility, SABR, volatility cube, swaption
(12 pages, 2011)

203. J.-P. Kreiss, T. Zangmeister
Quantification of the effectiveness of a safety function in passenger vehicles on the basis of real-world accident data
Keywords: logistic regression, safety function, real-world accident data, statistical modeling
(23 pages, 2011)

204. P. Ruckdeschel, T. Sayer, A. Szimayer
Pricing American options in the Heston model: a close look on incorporating correlation
Keywords: Heston model, American options, moment matching, correlation, tree method
(30 pages, 2011)

205. H. Ackermann, H. Ewe, K.-H. Küfer, M. Schröder
Modeling profit sharing in combinatorial exchanges by network flows
Keywords: Algorithmic game theory, profit sharing, combinatorial exchange, network flows, budget balance, core
(17 pages, 2011)

206. O. Iliev, G. Printsypar, S. Rief
A one-dimensional model of the pressing section of a paper machine including dynamic capillary effects
Keywords: steady modified Richards' equation, finite volume method, dynamic capillary pressure, pressing section of a paper machine
(29 pages, 2011)

207. I. Vecchio, K. Schladitz, M. Godehardt, M. J. Heneka
Geometric characterization of particles in 3d with an application to technical cleanliness
Keywords: intrinsic volumes, isoperimetric shape factors, bounding box, elongation, geodesic distance, technical cleanliness
(21 pages, 2011)

208. M. Burger, K. Dreßler, M. Speckert
Invariant input loads for full vehicle multibody system simulation
Keywords: multibody systems, full-vehicle simulation, optimal control
(8 pages, 2011)

209. H. Lang, J. Linn, M. Arnold
Multibody dynamics simulation of geometrically exact Cosserat rods
Keywords: flexible multibody dynamics, large deformations, finite rotations, constrained mechanical systems, structural dynamics
(28 pages, 2011)

210. G. Printsypar, R. Ciegis
On convergence of a discrete problem describing transport processes in the pressing section of a paper machine including dynamic capillary effects: one-dimensional case
Keywords: saturated and unsaturated fluid flow in porous media, Richards' approach, dynamic capillary pressure, finite volume methods, convergence of approximate solution
(24 pages, 2011)

211. O. Iliev, G. Printsypar, S. Rief
A two-cimensional model of the pressing section of a paper machine including dynamic capillary effects
Keywords: two-phase flow in porous media, steady modified Richards' equation, finite volume method, dynamic capillary pressure, pressing section of a paper machine, multipoint flux approximation
(44 pages, 2012)

212. M. Buck, O. Iliev, H. Andrä
Multiscale finite element coarse spaces for the analysis of linear elastic composites
Keywords: linear elasticity, domain decomposition, multiscale finite elements, robust coarse spaces, rigid body modes, discontinuous coefficients
(31 pages, 2012)

Status quo: April 2012